

AD-A045 280

ANALYSIS AND COMPUTER SYSTEMS INC BURLINGTON MASS  
ANALYTICAL AND PROCESSING SYSTEMS FOR ROCKET AND BALLOON PROBE --ETC(U)  
APR 77 H L DOLAN, C LIN, C TSAI

F/G 4/1

F19628-74-C-0169

UNCLASSIFIED

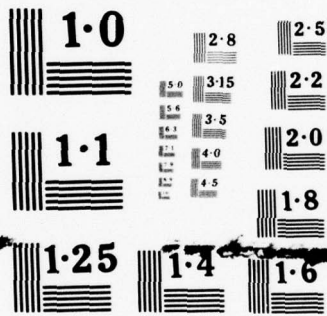
AFGL -TR-77-0101

NL

OF  
ADA  
045280



END  
DATE  
FILMED  
11-77  
DDC



NATIONAL BUREAU OF STANDARDS  
MICROCOPY RESOLUTION TEST CHART

AD A 045280

AFGL-TR-77-0101

9  
B.S.

ANALYTICAL AND PROCESSING SYSTEMS FOR ROCKET AND BALLOON PROBE DATA

Harold L. Dolan, III  
Ching-Lan Lin  
Chung-Jen Tsai

Analysis & Computer Systems, Inc.  
109 Terrace Hall Avenue  
Burlington, Massachusetts 01803

April 1977

Final Report for Period 1 April 1976 - 31 March 1977

Approved for public release; distribution unlimited

AU NO. \_\_\_\_\_  
DDC FILE COPY

Prepared for

AIR FORCE GEOPHYSICS LABORATORY  
AIR FORCE SYSTEMS COMMAND  
UNITED STATES AIR FORCE  
HANSCOM AFB, MASSACHUSETTS 01731

DDC  
RECEIVED  
OCT 14 1977  
D

Qualified requestors may obtain additional copies from the Defense Documentation Center. All others should apply to the National Technical Information Service.

Unclassified

SECURITY CLASSIFICATION OF THIS PAGE (When Data Entered)

REPORT DOCUMENTATION PAGE		READ INSTRUCTIONS BEFORE COMPLETING FORM
1. REPORT NUMBER <b>18</b> AFGL TR-77-0101	2. GOVT ACCESSION NO.	3. RECIPIENT'S CATALOG NUMBER <b>96</b>
4. TITLE (and Subtitle) Analytical and Processing Systems for Rocket and Balloon Probe Data.		5. TYPE OF REPORT & PERIOD COVERED Final Report, <del>Unpublished</del> 1 April 1976 - 31 March 1977
7. AUTHOR(s) <b>10</b> Harold L. Dolan, III, Ching-Lan/Lin Chung-Jen/Tsai		8. CONTRACT OR GRANT NUMBER(s) <b>15</b> F19628-74-C-0169 ✓
9. PERFORMING ORGANIZATION NAME AND ADDRESS Analysis & Computer Systems, Inc. ✓ 109 Terrace Hall Avenue Burlington, Massachusetts 01803		10. PROGRAM ELEMENT, PROJECT, TASK AREA & WORK UNIT NUMBERS N/A
11. CONTROLLING OFFICE NAME AND ADDRESS Air Force Geophysics Laboratory (SU YA) Hanscom Air Force Base, Massachusetts 01731 Contract Monitor: Robert McInerney (SU YA)		12. REPORT DATE <b>11</b> April 1977
14. MONITORING AGENCY NAME & ADDRESS (if different from Controlling Office)		13. NUMBER OF PAGES <b>12</b> 55 P.
		15. SECURITY CLASS. (of this report) Unclassified
		15a. DECLASSIFICATION/DOWNGRADING SCHEDULE
16. DISTRIBUTION STATEMENT (of this Report)  A - Approved for public release; distribution unlimited		
17. DISTRIBUTION STATEMENT (of the abstract entered in Block 20, if different from Report)		
18. SUPPLEMENTARY NOTES  TECH, other		
19. KEY WORDS (Continue on reverse side if necessary and identify by block number) Absorption Cross Section      Electron Accelerator      Jacchia Model Absorption Spectroscopy      Electron Practical Range      Luminous Efficiency Altimeter      Extinction Coefficient      Nephelometer Angular Response Function      Intensity Profile      Number Density Aspect Modulation      Intensity Ratio      Optical Emission		
20. ABSTRACT (Continue on reverse side if necessary and identify by block number) This report describes a number of numerical and processing procedures that were developed to aid Air Force Geophysics Laboratory (AFGL) researchers in the analysis and interpretation of experimental data. The research areas for which these techniques were developed include: The determination of the number densities of atmospheric constituents by the technique of absorption spectroscopy, balloon-borne nephelometer measurements of atmospheric aerosol properties, and the study of induced atmospheric optical emissions by rocket-borne electron accelerators.		

DD FORM 1 JAN 73 1473

EDITION OF 1 NOV 65 IS OBSOLETE

Unclassified

SECURITY CLASSIFICATION OF THIS PAGE (When Data Entered)

403410

~~Unclassified~~

SECURITY CLASSIFICATION OF THIS PAGE(When Data Entered)

19. KEY WORDS (Continued)

Polarization Ratio  
Solar Aspect Angle  
Solar Aspect Sensor  
Solar Zenith Angle  
Telephotometer  
Volume Scattering Function

Unclassified

SECURITY CLASSIFICATION OF THIS PAGE(When Data Entered)

PREFACE

The technical efforts discussed in this report have been performed for the Analysis and Simulation Branch (SUYA) under contract number F19628-74-C-0169. This contractual effort consists of the design and development of analytical routines and logical techniques necessary for the reduction of raw digital data telemetered from rocket borne transducers to physical parameters required for experimental evaluation. The techniques to be developed will be applied to the analysis of PCM, PDM and FM data transmitted from (1) UV photometers, (2) EUV monochromators, (3) solar EUV scanning monochromators and (4) Laser monitor probes among others.

The analysis and mathematical techniques described in this report represent only certain phases of the research being conducted in the given areas.

The authors want to thank the Contract Monitor, Mr. Robert McInerney, Analysis and Simulation Section (SUYA), AFGL Computation Branch, Air Force Geophysics Laboratory; Mr. Frank Gibson, Atmospheric Optics Branch, Optical Physics Division, AFGL; Mr. Robert O'Neil, Radiation Effects Branch (OPR), Optical Physics Division, AFGL; and Mr. Lawrence Weeks, Atmospheric Structures Branch (LKB), Aeronomy Division, AFGL, whose expertise and technical guidance were of great assistance in the preparation of this report.

ACCESSION for	
NTIS	White Section <input checked="" type="checkbox"/>
DDC	Buff Section <input type="checkbox"/>
UNANNOUNCED	<input type="checkbox"/>
JUSTIFICATION .....	
BY .....	
DISTRIBUTION/AVAILABILITY CODES	
Dist.	AVAIL. and/or SPECIAL
A	

DDC  
RECEIVED  
OCT 14 1977  
RECEIVED  
D

TABLE OF CONTENTS

<u>Section</u>		<u>Page</u>
	PREFACE	3
	LIST OF ILLUSTRATIONS	6
1.0	INTRODUCTION	7
2.0	A PROCESSING SYSTEM FOR RESPONSE DATA FROM PRECESSING SOLAR RADIATION DETECTORS	8
3.0	DETERMINATION OF ATMOSPHERIC AEROSOL SCATTERING PROPERTIES FROM BALLOON-BORNE NEPHELOMETER DATA	27
4.0	A PROCESSING SYSTEM FOR ROCKET-BORNE ELECTRON ACCELERATOR EXPERIMENT DATA	42

LIST OF ILLUSTRATIONS

<u>Figure</u>		<u>Page</u>
2.1	Preliminary Data Reduction	10
2.2	Snapshot Plot	13
2.3	Solar Aspect Sensor (a) Diamond-Shaped Aperture (b) Output Signal	15
2.4	Aspect Sensor Data Processing	16
2.5	Pulse Train Telemetered from the Aspect Sensor	17
2.6	Aspect Angle and Fitted Curve	19
2.7	Aspect Angle Corrections to Sensor Voltages	22
2.8	Correction Factor Curve	25.
2.9	Final Corrected Sensor Profile	26
3.1	Nephelometer Data Processing System	28
3.2	Printout of Digitized Nephelometer Data	32
3.3	Nephelometer Data Stripchart	33
3.4	Nephelometer Data Profile Illustrating Gain Change	37
3.5	100 Deg. Volume Scattering Function vs. Altitude at 0.475(H) Micron	39
3.6	100 Deg. Polarization Ratio vs. Altitude at .475 Micron	40
3.7	Forward-To-Back Scatter Ratio at .475(V) Micron vs. Altitude	41
4.1	Flow Diagram of the Processing System for the Electron Accelerator Experiment Data	44
4.2	Staircase Potential Used for Calibrating the Digital Data	46
4.3	Time Dependent Telephotometer Data (a) 3914A <sup>o</sup> Data, (b) 5577A Data	49
4.4	Precede Measurement of N <sub>2</sub> <sup>+</sup> 1N 3914A <sup>o</sup> Luminous Efficiency	55

## 1.0 INTRODUCTION

This report describes a number of numerical and processing procedures that were developed to aid Air Force Geophysics Laboratory (AFGL) researchers in the analysis and interpretation of experimental data. The research areas for which these techniques were developed include: The determination of the number densities of atmospheric constituents by the technique of absorption spectroscopy, balloon-borne nephelometer measurements of atmospheric aerosol properties, and the study of induced atmospheric optical emissions by rocket-borne electron accelerators.

The processing systems discussed in this report are comprised of a number of program modules which have been documented and submitted separately. Copies of these programs and the intermediate data bases can be obtained by contacting the Analysis and Simulation Branch (SUYA) of Air Force Geophysics Laboratory.

## 2.0 A PROCESSING SYSTEM FOR RESPONSE DATA FROM PRECESSING SOLAR RADIATION DETECTORS

Rocket measurements of the number densities of ozone ( $O_3$ ) and molecular oxygen ( $O_2$ ) are being performed in the upper atmosphere by the technique of absorption spectroscopy. These measurements are made aboard sounding rockets by several solar radiation detectors, (or "sensors"), each sensitive to a particular wavelength of radiation. The radiation intensity as measured by these sensors is constantly telemetered to the earth as the rocket passes through the earth's atmosphere. Absorption profiles of each wavelength are obtained by methods to be described. These profiles are used to deduce the number densities of the atmospheric constituents of interest.

Certain wavelengths of solar radiation are absorbed only by particular atmospheric constituents. This is because at these wavelengths the absorption cross sections for these species are much higher than for others. (The absorption cross section of a material is a measure of the probability of absorption of radiation). For example, at the wavelengths 2600Å and 2750Å the absorption cross section for ozone is much higher than for molecular oxygen and the other major atmospheric constituents. Similarly at the wavelength 1216Å (corresponding to the Lyman- $\alpha$  line of hydrogen in the solar spectrum) only molecular oxygen is a significant absorber.

This experiment exploits this phenomenon by measuring the altitude profile of the radiation intensities at these wavelengths. The number densities of the principle absorbers are then inferred as follows. If  $I(\lambda, Z)$  is the intensity of wavelength  $\lambda$  radiation at altitude  $Z$ , and if  $\lambda$  corresponds to a wavelength for which the absorption cross section  $\sigma(\lambda)$ , is significant for only one atmospheric species, then the altitude profile of the number density of this species is given by:

$$n(Z) = \frac{1}{\sec \chi \sigma(\lambda)} \frac{d}{dz} \text{Log } I(\lambda, Z)$$

where  $\chi$  is the solar zenith angle. The solar radiation detectors employed in this experiment are sensitive only to these wavelengths. The radiation intensities of these wavelengths are measured at many altitudes and the intensity profile so determined is used in the equation above to obtain the number density of the particular atmospheric species.

The data so obtained must undergo extensive processing before it is of any use to the researcher. The data must be corrected for the precessing of the rocket, random background radiation, errors incurred in the data transmission, etc. The purpose of this processing is to reduce the sensor readings to a data file consisting of radiation intensity (for each wavelength), rocket spin rate and solar aspect angle at each altitude of the rocket flight (there will be approximately five (5) such data points per second. Typical rocket flights produce about 300 seconds of data). The data are then used by the researcher

in various atmospheric studies. The processing undergone by these data are described in the following sections.

## 2.1 Preliminary Data Reduction

The experiment packages carried aboard these sounding rockets usually employ two telemetry links to the ground recording stations. One link telemeters the output of the solar aspect sensor, and the other transmits the outputs of the various photon detectors. The latter makes use of the FM/FM type modulation, which permits the simultaneous transmission of the outputs of several transducers. Usually eight of these "telemetry channels" are reserved for the outputs of the photon detectors. The detectors are arranged in pairs mounted 180° apart in the payload. The outputs of both detectors of a pair are wired in parallel and telemetered through a single channel. This "time-multiplexing" of the sensors halves the number of telemetry channels required for the photon detectors. Since the outputs are weak at low altitudes, these outputs are further amplified by a factor of ten and telemetered on another channel.

The resulting experiment data consist of the time varying solar aspect sensor output, and the eight time varying detector outputs, and are recorded on magnetic tape in analog form at the launch site. Later they are digitized by the AFGL Decommutation Branch, using either the Astrodata or the Honeywell H-316 A/D systems. The processing system described in this section begins with these digital tapes. Since the format of these tapes is not directly compatible with the CDC 6600, modular routines were written to read, unpack and convert the data to a format which can be used by the FORTRAN programs which comprise this processing system.

### 2.1.1 Raw Data Display

The flow of the initial data reduction is illustrated in Figure 2.1. Verification of the experimental data is done first by obtaining plots and printouts of the digitized data tapes (digital counts vs. elapsed time for each sensor). The researcher is given a set of these listings and plots for a preliminary review. The plots can be compared with analog strip charts, recorded at launch time, and it can be ascertained whether or not the digitization was done properly. The researcher may identify possible sensor malfunctions, telemetry noise and background levels. His analysis of the data may result in processing the data with filtering or smoothing routines, or completely ignoring any work effort for a particular sensor.

### 2.1.2 Pulse Identification and Reduce

Most of the sensor signatures recorded in experiments of this type are in the form of a series of pulses which rise above non-event periods called background. In this experiment the pulses occur once every rotation of the rocket, the peak occurring when the sensor is closest to the sun, and the background when the sun is outside the sensor's field of view. The

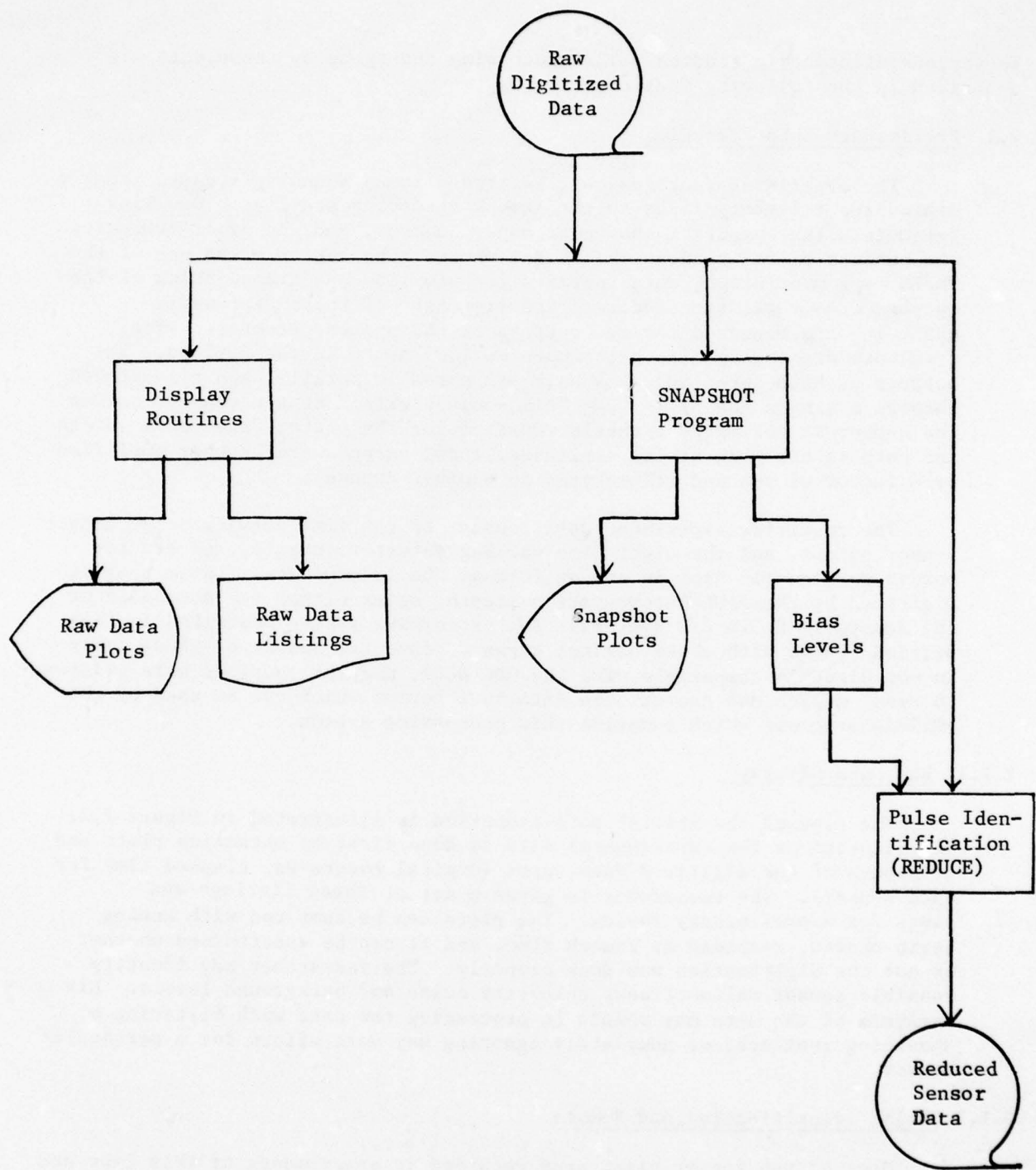


Figure 2.1 Preliminary Data Reduction

REDUCE program is used to reduce the amount of data to be handled to a more practical level, by extracting the pulses. In some applications the shapes of the pulses are important so that all the points comprising each pulse are saved along with the corresponding pulse start and stop times. In all cases the points which define a pulse outline are differentiated from background or noise. This is accomplished by choosing an appropriate "bias" level, slightly above the background level, points above which are considered to be part of a pulse.

The logic for pulse identification requires the accurate definition of several parameters. Extensive analysis of the plots and listings of the raw digitized data from several sections of the flight is necessary to assure the universality of these parameters. The choice of these parameters, particularly the bias level, often is made in conjunction with the running of the SNAPSHOT program, described below. The parameters to be defined are: The background level, the bias level, the minimum number of points in a pulse (NMIN) and the maximum number of points in a pulse (NMAX). In some cases the file must be processed defining these parameters differently for different segments of the data.

The logic assumes that the first data samples interrogated are background samples. Consequently, an appropriate elapsed time must be chosen for initial processing. The module has the option of averaging all samples between pulses to define the background, to include the last N samples as a running average background, (where N is determined by the sample rate), or using a constant background, determined by the user.

Since a certain amount of jitter or noise must be anticipated, another parameter included is the number of counts a sample must exceed before being considered the possible beginning of a pulse (NMIN). Minimizing this threshold is essential if the pulses do not rise far above the background or if the pulse width is a desired result. Once the sample count exceeds the bias, NMIN consecutive samples must exceed the bias. If the sample count drops below the bias before NMIN counts have been found, the search begins again. This check eliminates spurious noise spikes which can exceed the bias value, but which usually are not of sufficient width to fulfill the NMIN consecutive samples criterion.

If the criterion is satisfied, consecutive samples are considered to be part of the pulse until NMIN consecutive samples are below the threshold value. If the total number of samples defined to be part of the pulse exceed NMAX, the pulse is not saved and the data are interrogated but not saved until the sample counts fall below the bias value. This check eliminates areas with extensive noise. If the pulse width is a variable, the value of NMAX must be greater than the number of samples in the widest pulse.

Once a pulse has been identified, the average preceding background level, number of samples in the background, number of samples in the pulse, start and stop times of the pulse and an array containing the samples in

the pulse are returned to the calling module. This module is successively called for each pulse in the sensor data until a reduced data file is created. One such data file is created for each telemetry channel (including aspect). Sometimes several of these files are retained on a single reel of magnetic tape.

### 2.1.3 SNAPSHOT Fit

The SNAPSHOT program provides an independent check on the choice of the above parameters. This program displays, one pulse per frame, the points in a pulse, noting the bias and background levels. The data are plotted on an expanded scale, where it is easy to determine if these levels have been defined correctly. An example of a SNAPSHOT plot is given in Figure 2.2.

Once a pulse has been identified, it is then necessary to determine the peak voltage in it. This is done later by the SENSAR program by fitting a parabola to the points in the pulse. The maximum value of the parabola is taken as the peak voltage for that pulse. Not all the points are used in the fit, but only a certain number above and below the center of the pulse. This number is also determined with the assistance of the SNAPSHOT program. This program displays, one pulse per frame, the points in a pulse, and the parabola fitted to those points. The peak voltage is also noted.

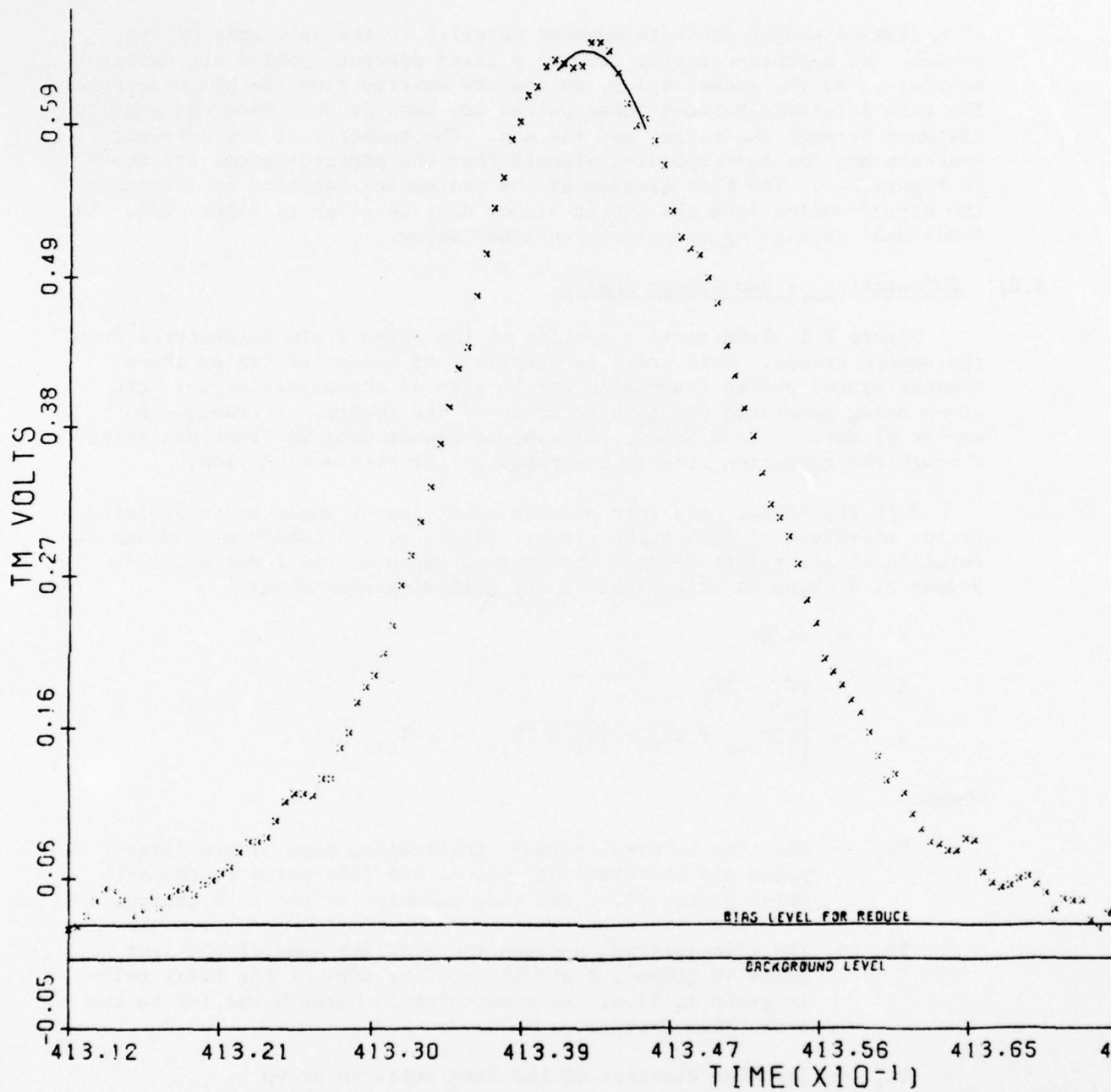
This routine can be used to examine data from tapes created on either the Astrodata or Honeywell systems. Thus the rate of digitization, the peak fit, and the bias and background level voltages can be examined in one intermediate processing step.

## 2.2 Aspect Determination

The sensitivity of the radiation detectors used in these experiments varies with the angle of incidence of the radiation impinging upon them. The detector sensitivities are maximum at normal incidence, and decrease monotonically as the angle becomes more oblique. The sensitivity is dependent upon many factors such as the detector type and geometry, the thickness and composition of the window, etc., and usually is different for each individual instrument.

This phenomenon would be of no consequence here if the photon detectors were pointed continuously at the sun, as is possible in some satellite and large rocket applications. However, the precessional motion of small sounding rockets, such as the Nike Apache used in this type of experiment, can cause off-axis measurements as high as  $20^\circ$ . For this reason the experiment payloads are equipped with solar aspect sensors, the data from which are used to determine the angular sensitivities of the detectors, and to correct for conditions of normal incidence.

The solar aspect sensor is a device which determines the angle between the spin axis of the rocket and the rocket-sun line. The detector consists



PEAK = .64419

Figure 2.2 SNAPSHOT Plot

of a diamond-shaped aperture mounted parallel to the spin axis of the rocket, and a photo-detector located a fixed distance behind the detector aperture. As the rocket spins, pulses are emitted from the photo-detector. The time intervals between these pulses are used to determine the angular distance between the rocket and the sun. The geometry of the detector aperture and the corresponding signals from the photo-detector are shown in Figure 2.3. The flow diagram of the processing required to determine the aspect angles from the aspect sensor data is given in Figure 2.4. The individual processing steps are described below.

### 2.2.1 Calculation of Raw Aspect Angles

Figure 2.5 illustrates a section of the pulse train telemetered from the aspect sensor. This train is comprised of groups of two or three closely spaced pulses (depending on the sign of the aspect angle), one group being generated for each rotation of the rocket. To reduce the amount of data to be handled, this aspect sensor data is first processed through the reduction program described in the previous section.

Both the rocket spin rate and the solar aspect angle are calculated at the mid-times of each pulse group. First,  $\phi$ , the number of radians of rotation of the rocket between the leading edges of the first and last pulses of a group is calculated by the following equations:

$$\begin{aligned}\phi &= (A/B)\pi \\ A &= TG_i - TL_i \\ B &= \left[ \frac{1}{2}TG_{i-1} + TB_i + TG_i + TB_{i+1} + \frac{1}{2}TG_{i+1} \right] / 2\end{aligned}$$

where:

$TG_i$  = The time interval between the leading edge of the first pulse and the trailing edge of the last pulse in the  $i$ -th pulse group, (i.e. the time duration of the  $i$ -th group).

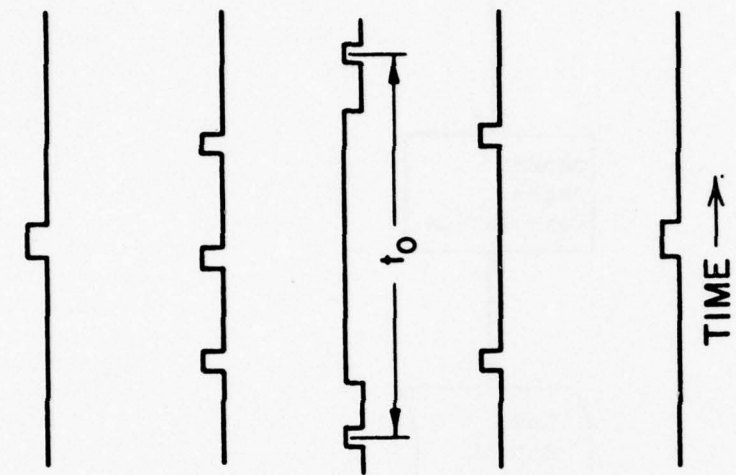
$TB_i$  = The time interval between the trailing edge of the last pulse in group  $i-1$  and the leading edge of the first pulse in group  $i$ , (i.e. the time duration between the  $i-1$  to the  $i$ -th pulse groups).

$TL_i$  = The time duration of the last pulse in group  $i$ .

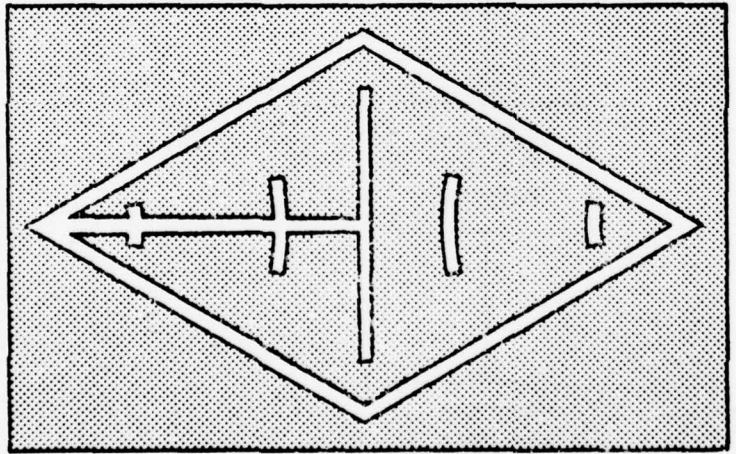
therefore:

$A$  = The time interval between the leading edges of the first and last pulses of the  $i$ -th group.

$B$  = The rotational period of the rocket at the center of group  $i$ .



(b)



(a)

$\alpha$  (POSITIVE)  
 $\alpha = 0^\circ$   
 $\alpha$  (NEGATIVE)

Figure 2.3 Solar Aspect Sensor  
 (a) Diamond-shaped aperture  
 (b) Output signal

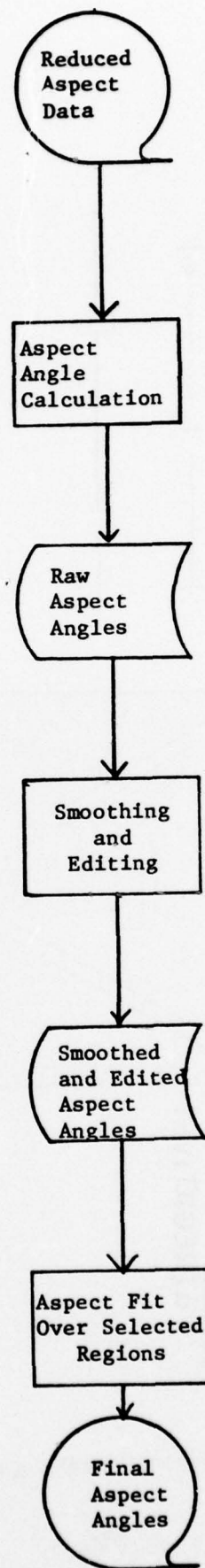


Figure 2.4 Aspect Sensor Data Processing

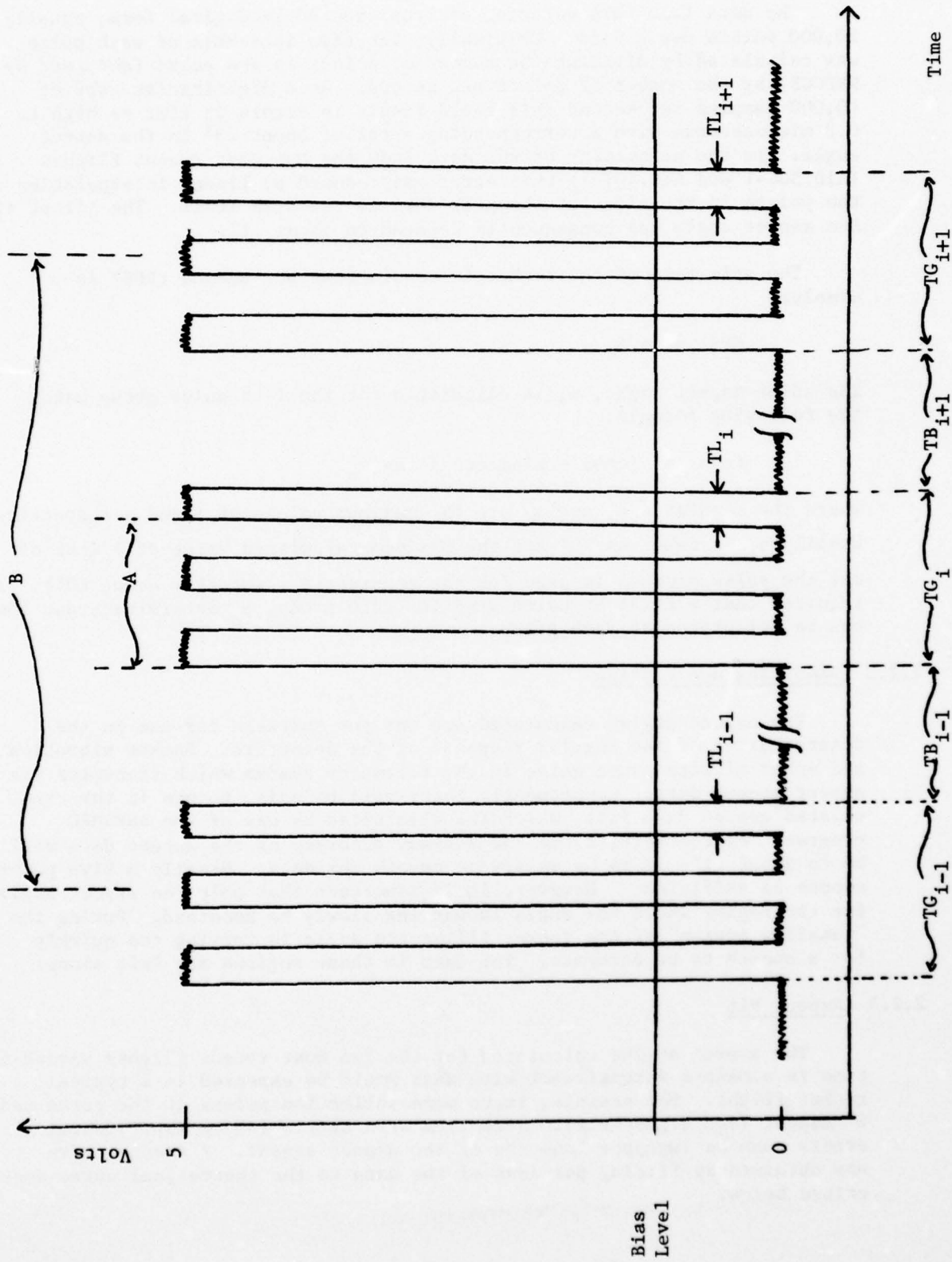


Figure 2.5 Pulse Train Telemetered from the Aspect Sensor

The data from this detector are represented in digital form, usually 10,000 points per second. Originally, the time intervals of each pulse was calculated by dividing the number of points in the pulse (obtained by REDUCE) by the number of points per second. At a digitization rate of 10,000 samples per second this could result in errors in time as high as 0.2 microseconds with a corresponding error of about  $.3^\circ$  in the aspect angle. In the processing of the data from the two most recent flights (A10.504-1 and A10.507-1) this error was reduced by linear interpolation of the points in the sides of the peak down to the bias level. The jitter in the aspect angle was consequently reduced to about  $.1^\circ$ .

The spin rate of the rocket in revolutions per second (RPS) is simply:

$$\text{RPS} = 1/B \quad .$$

The solar aspect angle,  $\alpha$ , is calculated for the  $i$ -th pulse group using the following formula:

$$\tan \alpha = (\cos \phi - \sin \phi \cot \phi_0) \tan \alpha_m$$

where the constants  $\phi_0$  and  $\alpha_m$  are the maximum values of  $\phi$  and  $\alpha$  respectively. Usually  $\alpha_m$  is taken as  $70^\circ$  and the maximum calculated value of  $\phi$  (out of all the pulse groups) is used for the constant  $\phi_0$ , (usually about  $60^\circ$ ). This requires that  $\phi$  first be calculated for each group,  $\phi_0$  determined, and then  $\alpha$  can be calculated at each group.

### 2.2.2 Smoothing and Editing

The aspect angles calculated are not yet suitable for use in the determination of the angular response of the detectors. Rocket vibration and other effects cause noise in the telemetry system which transmits the aspect sensor data. Consequently there will be noise points in the calculated aspect data file, which are eliminated by use of the ASPSMED program. Furthermore, since the maximum accuracy of the aspect data will be to about  $.1^\circ$ , it is necessary to smooth the data. Usually a five point smooth is sufficient. However, it is important that only the aspect angles for the region where the angle is varying slowly be smoothed. During the "tumbling region" of the rocket flight the angle is varying too quickly for a smooth to be accurate. The data in these regions are left alone.

### 2.2.3 Aspect Fit

The aspect angles calculated for the two most recent flights varied in time in a manner inconsistent with what would be expected in a typical rocket flight. For example, there were inflection points in the curve near  $0^\circ$  aspect (see Figure 2.6). Anomalies were attributed to experimental errors such as improper mounting of the aspect sensor. A smooth curve was obtained by fitting portions of the data to the theoretical curve described below.

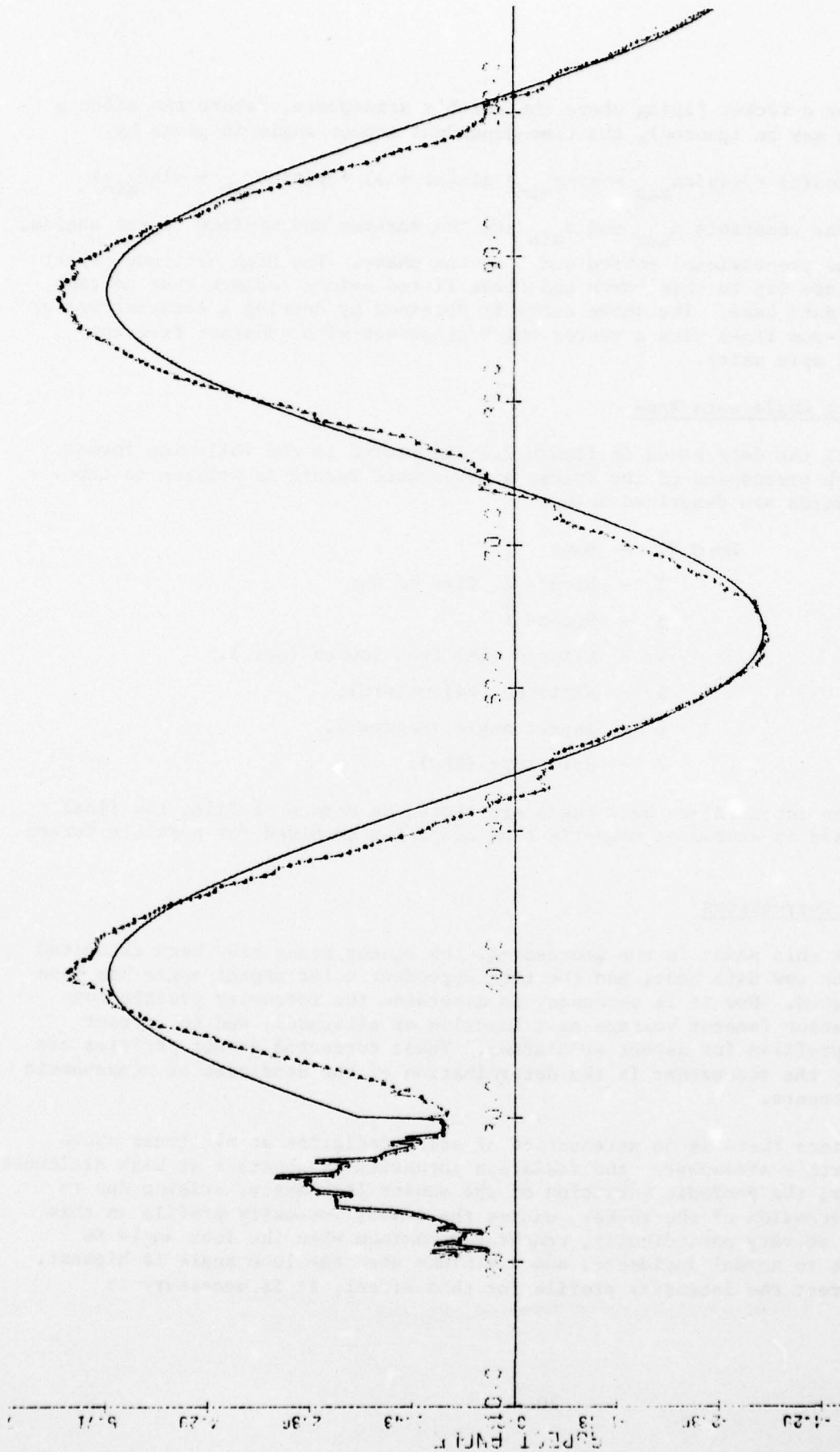


Figure 2.6 Aspect Angle and Fitted Curve

For a rocket flying above the earth's atmosphere, (where the effects of drag may be ignored), the time-dependent aspect angle is given by:

$$\sin\alpha(t) = \frac{1}{2}(\sin\alpha_{\max} - \sin\alpha_{\min}) \sin(\omega t + \phi) + \frac{1}{2}(\sin\alpha_{\max} + \sin\alpha_{\min})$$

where the constants  $\alpha_{\max}$  and  $\alpha_{\min}$  are the maximum and minimum aspect angles,  $\omega$  is the precessional period and  $\phi$  is the phase. The high altitude aspect angles are fit to this curve and these fitted points replace that portion of the data base. The above curve is obtained by dotting a constant vector (rocket-sun line) with a vector which precesses with constant frequency (rocket spin axis).

#### 2.2.4 Aspect Angle Data Base

All the data bases in Figure 2.4 are stored in the following format. For each precession of the rocket a seven word record is written to tape. These words are described below:

Word #1	- Hour	} Time of Day
2	- Minute	
3	- Second	
4	- Elapsed time from launch (sec.).	
5	- Altitude (kilometers).	
6	- Aspect angle (degrees).	
7	- Spin rate (RPS).	

The intermediate data bases are stored on permanent file, the final data base is stored on magnetic tape and later archived for possible future use.

#### 2.3 Sensor Corrections

At this point in the processing, the sensor peaks have been extracted from the raw data base, and the time dependent solar aspect angle has been calculated. Now it is necessary to determine the intensity profile for each sensor (sensor voltage as a function of altitude), and to correct these profiles for aspect modulation. These corrected sensor profiles are used by the researcher in the determination of the densities of atmospheric constituents.

Since there is no attenuation of solar radiation at altitudes above the earth's atmosphere, the radiation intensity is constant at high altitudes. However, the periodic variation of the sensor look angle, arising due to the precession of the rocket, causes the sensor intensity profile in this region to vary periodically, reaching a maximum when the look angle is closest to normal incidence, and a minimum when the look angle is highest. To correct the intensity profile for this effect, it is necessary to

determine the response of the detector, i.e. the amount of intensity deterioration as a function of look angle. This results in a correction factor vs. look angle curve for each sensor. These curves are applied to the sensor voltages and final data base of the corrected sensor voltages is created. The flow of this phase of the processing is illustrated in Figure 2.7, and described below.

### 2.3.1 Uncorrected Voltage Data Base

When analog data is digitized, voltages are represented as "digital counts". The lowest and highest digital counts refer to the lowest and highest analog voltages, respectively. For the data in this experiment, the telemetry voltages range from 0 to 5V, and the corresponding digital representations are -1638 counts and +1638 counts, respectively. To convert the digital data to volts, one simply multiplies each point by 5V/3276. The peak voltage in each pulse is determined by fitting a quadratic to the points in the pulse, and then solving this quadratic for the maximum voltage and corresponding time. The number of points to be used in the quadratic fit is determined earlier when running the SNAPSHOT program.

After the peak voltages have been determined there will be one data point for each rotation of the rocket. These data are merged with the solar aspect angles to create, for each telemetry channel, a file containing time, altitude, vehicle spin rate, sensor voltage and aspect angle. Since spin rate, aspect angles and sensor peak voltages are not available at precisely the same times, a Lagrangian interpolation scheme is used to estimate the aspect angle and spin rate at the times when the sensor voltage is at a peak. For each rotation of the rocket a nine word record is written to tape. The contents of these words are described below:

Word #1	= Hour	}	Time of Day.
2	= Minute		
3	= Second		
4	= Elapsed time from launch (sec.).		
5	= Altitude (km).		
6	= Aspect angle (deg).		
7	= Spin rate (RPS).		
8	= Sensor output (volts).		
9	= Sensor ID (1 or 2 corresponding to one of the two time - multiplexed sensors on this channel).		

This data base is retained as a system permanent file during the processing, and later is copied to a magnetic tape for archiving.

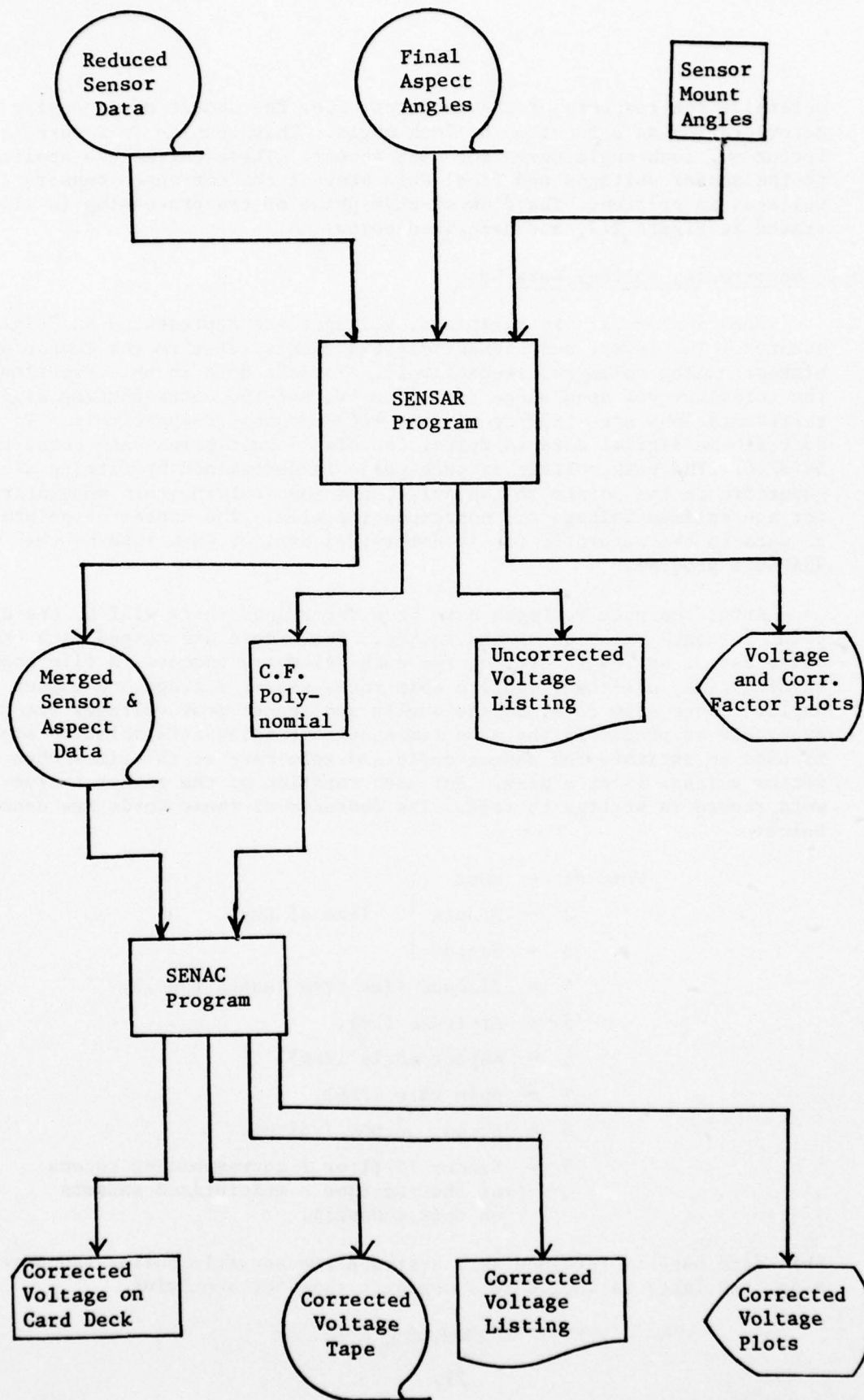


Figure 2.7 Aspect Angle Corrections to Sensor Voltages

### 2.3.2 Determination of Detector Response

The next step in the processing is to determine the sensor voltage profile which would result if the sensor were pointed continuously at the sun, that is, if there were no precession of the rocket. The sensor look angle,  $\beta$ , is defined as the angular deviation of the sensor from normal incidence. Mathematically:

$$\beta \equiv |\alpha - MA|$$

where  $\alpha$  is the aspect of the rocket, and MA is the mount angle of the particular sensor under consideration. The absolute value is taken because the detector response is independent of the sign of the look angle.

The mount angles are provided by measurements made on the sensors before flight. However, these measured angles are not precise due to experimental errors and flexing of the experiment payload during flight. Consequently the mount angles used may be slightly different from those measured.

The correction factor,  $cf(\beta)$ , for a given detector is defined as:

$$cf(\beta) = \frac{I_{\infty}(0)}{I_{\infty}(\beta)}$$

where  $I_{\infty}(0)$  is the intensity of the radiation above the earth's atmosphere, as measured by the detector when it is normal to the radiation, and  $I_{\infty}(\beta)$  is the intensity measured when the detector is at look angle  $\beta$ .  $cf(\beta)$  is a monotonically increasing function of  $\beta$ , and is independent of altitude. The correction factor is used to correct an intensity measurement (at any altitude), by a detector at an angle  $\beta$  from normal incidence to what would have been measured had the detector been situated normal to the incoming radiation. During this phase of the processing, the sensor output data are combined with the calculated solar aspect angles to obtain an estimate of  $cf(\beta)$  for each radiation detector used in the experiment. Later these will be used to correct the detector outputs for aspect modulation.

It is necessary to determine the voltage which would be output by each sensor when it is at high altitudes, (where there is no atmospheric attenuation), and normal to the incoming solar radiation. The actual voltages measured at these altitudes oscillates between a high and low value, as the look angle oscillates due to the precession of the rocket, the peak voltage at each precession cycle being observed when  $\beta = 0$ . A few of the peak voltages measured at high altitudes when  $\beta \approx 0$  are averaged and saved along with the corresponding times. A quadratic equation (call it  $V_0(t)$ ) is fit to these points. This quadratic is the approximation to the voltage which would be measured if the detector was always normal to the radiation. For most detectors  $V_0(t)$  would be simply a constant, but a

quadratic is used because the 1450Å radiation is still slightly attenuated at the highest altitudes attained by the rocket.

The next step is to form the ratio  $V_o(t)/V(t)$ , at times corresponding to high altitudes, where  $V(t)$  is the measured voltage at time  $t$ . This ratio will be close to unity near 0° look angle and will become larger as the look angle increases. This reflects the fact that a larger correction is required as the angle between the experiment sensor and the solar radiation increases. These ratios are calculated only at high altitudes where only the look angle affects the measured voltage.

These ratios are plotted against mount angle (Figure 2.8). Since the rocket has precessed several times during the times over which these ratios were calculated, there will be several ratios for each value of the look angle. The variance of these ratios will depend on the accuracy of the mount angle used. Usually the above procedure is repeated using several mount angles, and the mount angle which results in the least amount of scatter in the ratio plots is used. A polynomial is fit to these ratios, and this constitutes the approximation to the function  $cf(\beta)$ .

The SENSAR program is used for both merging the sensor voltage with the aspect angles, and the determination of the correction factor. The SENAC program, described below combines these to create the final corrected voltages for each experiment sensor.

### 2.3.3 Application of Correction Factors

Now that the correction factor polynomial has been determined, and the sensor voltage data base created, it is a simple matter to apply the correction factor to the measured voltages to obtain the corrected sensor profiles. Each sensor reading is multiplied by the appropriate correction factor to give the final corrected voltage. Since the polynomial approximation is used, all voltages with the same look angle will be multiplied by the same ratio.

The aspect and sensor deterioration corrected voltages are plotted against elapsed time. Figure 2.9 is an example of a corrected voltage plot. If the corrections are applicable, the corrected voltage profile should be a horizontal line at times when the rocket is above the earth's atmosphere. The only variations from this horizontal line should be minor jitter attributable to sensor sensitivity. The corrected voltages for each of the two sensors are punched on data cards and further subdivided into ascent and descent sections of the flight.

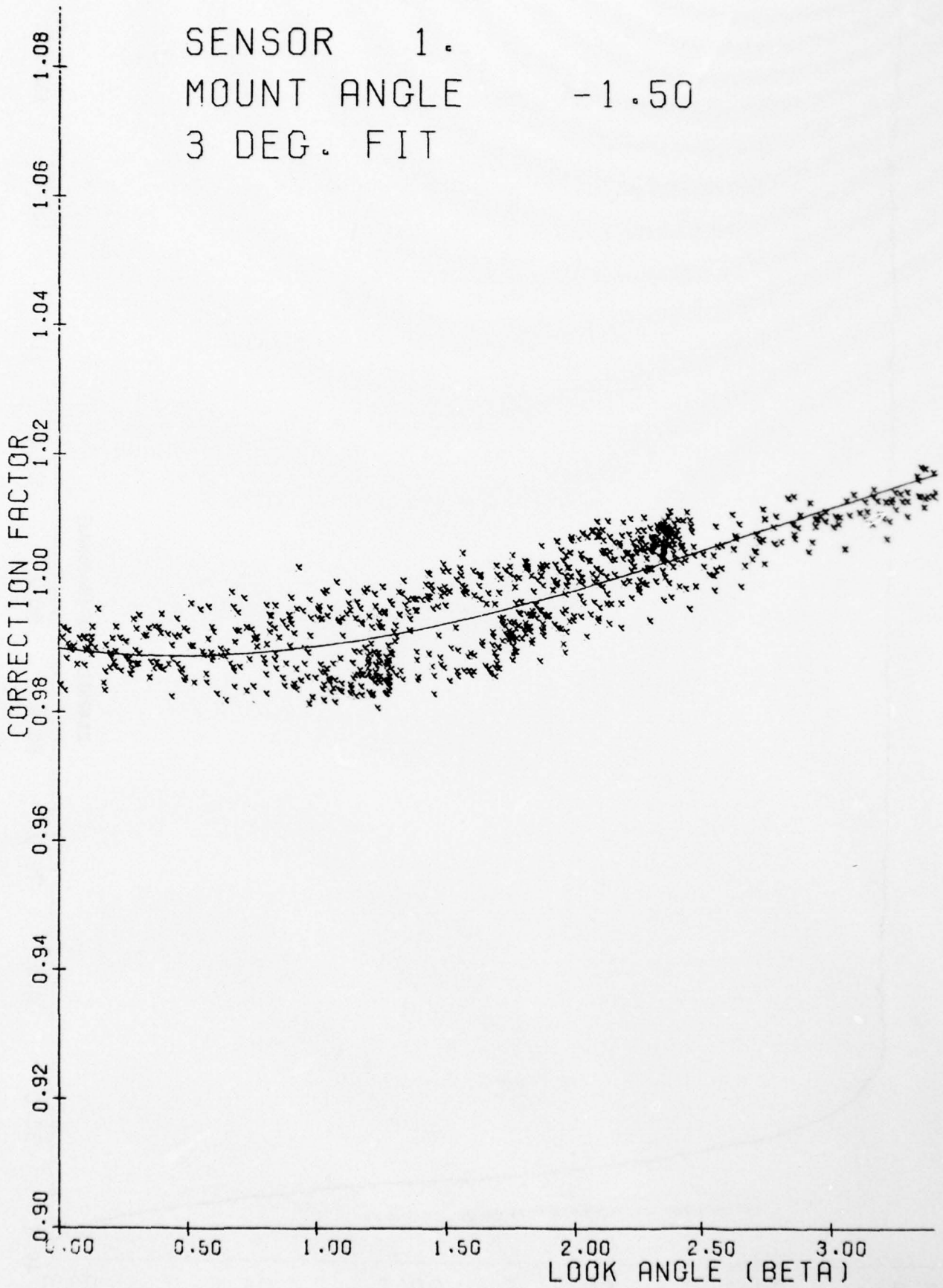


Figure 2.8 Correction Factor Curve

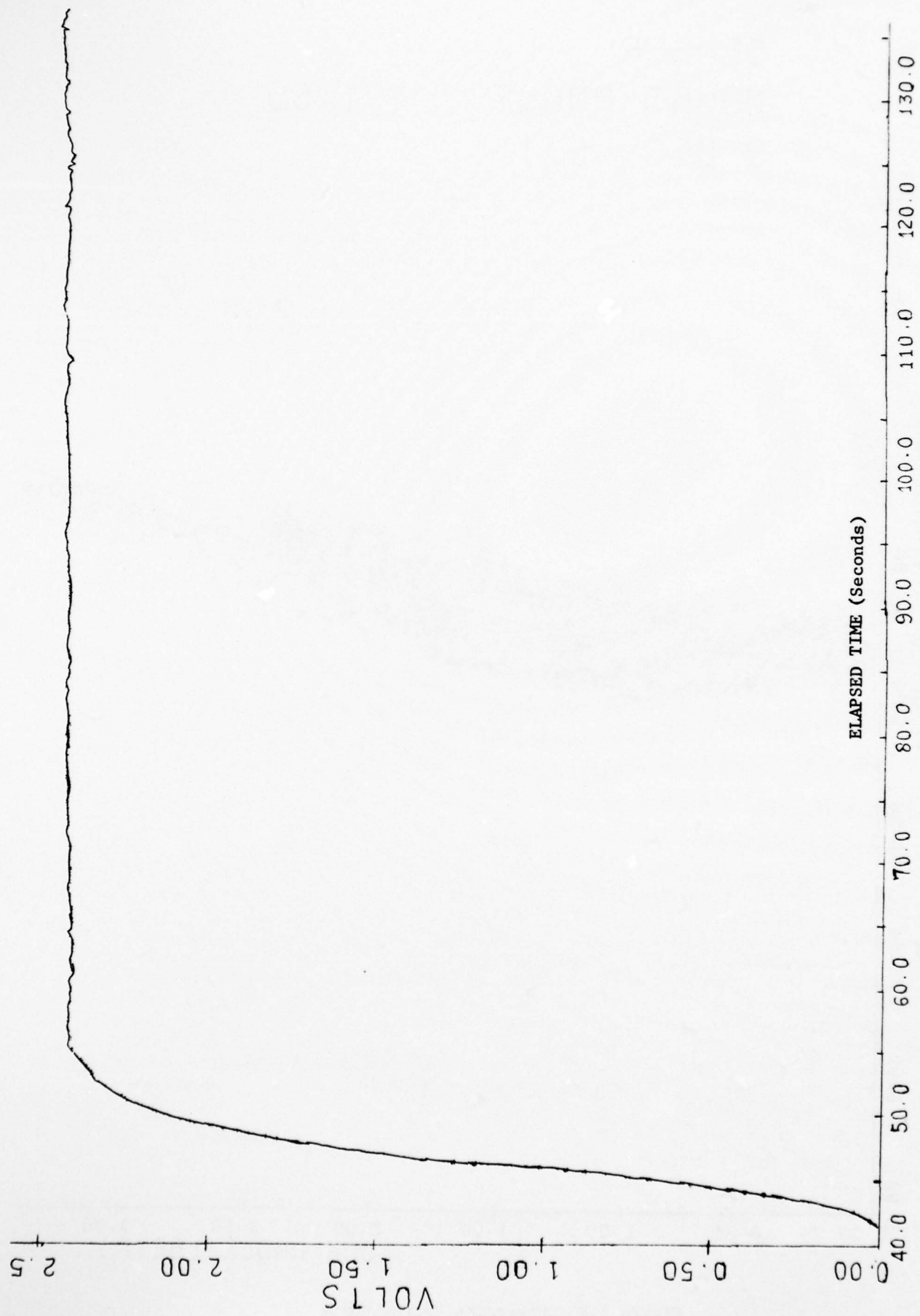


Figure 2.9 Final Corrected Sensor Profile

### 3.0 DETERMINATION OF ATMOSPHERIC AEROSOL SCATTERING PROPERTIES FROM BALLOON-BORNE NEPHELOMETER DATA

Experimental studies have revealed the existence of optical scattering properties in the atmosphere. Experiments by Gibson (Ref. 1), involving balloon-borne nephelometers, have been undertaken to study these properties. The optical scattering properties are usually determined from measurements of the extinction coefficient and the angular volume scattering function  $\beta(\phi)$ , where  $\phi$  is the scattering angle. The wavelength, polarization, and angular dependence of the scattered light are dependent upon optical and physical properties of air molecules and aerosol properties contained in the volume element. These properties include: particle size, distribution, refractive index and particle shape. They are proportional to molecular and aerosol number densities.

The determination of the angular volume scattering function,  $\beta(\phi)$ , as a function of altitude is accomplished by experiments involving balloon-borne nephelometers. The instrument measures  $\beta(\phi)$  in absolute quantities at five scattering angles for wavelengths in the visible spectrum. The polarization of the scattered light is analyzed at selected angles and wavelengths.

Theoretically, if the instrument response to energy reception is linear and  $\beta(\phi)$  the only remaining variable, then the response can be expressed as

$$W(\phi_s) = K\beta\lambda(\phi_s)$$

where  $K$  is the calibration factor for a photometer at scattering angle  $\phi_s$  and spectral filter of wavelength  $\lambda$ . After determination of  $K, \beta\lambda(\phi_s)$  is calculated as a function of altitude from the measured analog signal voltages from the nephelometer.

On the balloon-borne nephelometer, five photometers are mounted. The photometers measure scattered light from a defined volume of atmosphere at  $150^\circ$ ,  $100^\circ$ ,  $50^\circ$ ,  $30^\circ$ , and  $15^\circ$ . Adjacent to the aperture of each photometer is an eight-position filter wheel, which is rotated stepwise so as to provide a sampling of several spectral frequencies. Some filters have linear polarizers for certain photometers. These allow analysis of the perpendicular and parallel polarization of the scattered light.

Understanding of the purpose of the experiment, the form of the data, the intermediate stages in the processing stream, the anticipated results, and the formats of data representation leads to successful and accurate processing of the experimental data. The phases in the processing system are described in the following sections. The flow diagram for this system is given in Figure 3.1.

1. F. W. Gibson, "In Situ Photometric Observations of Angular Scattering from Atmospheric Aerosols," Applied Optics, Vol. 15, P. 2520, October 1976.

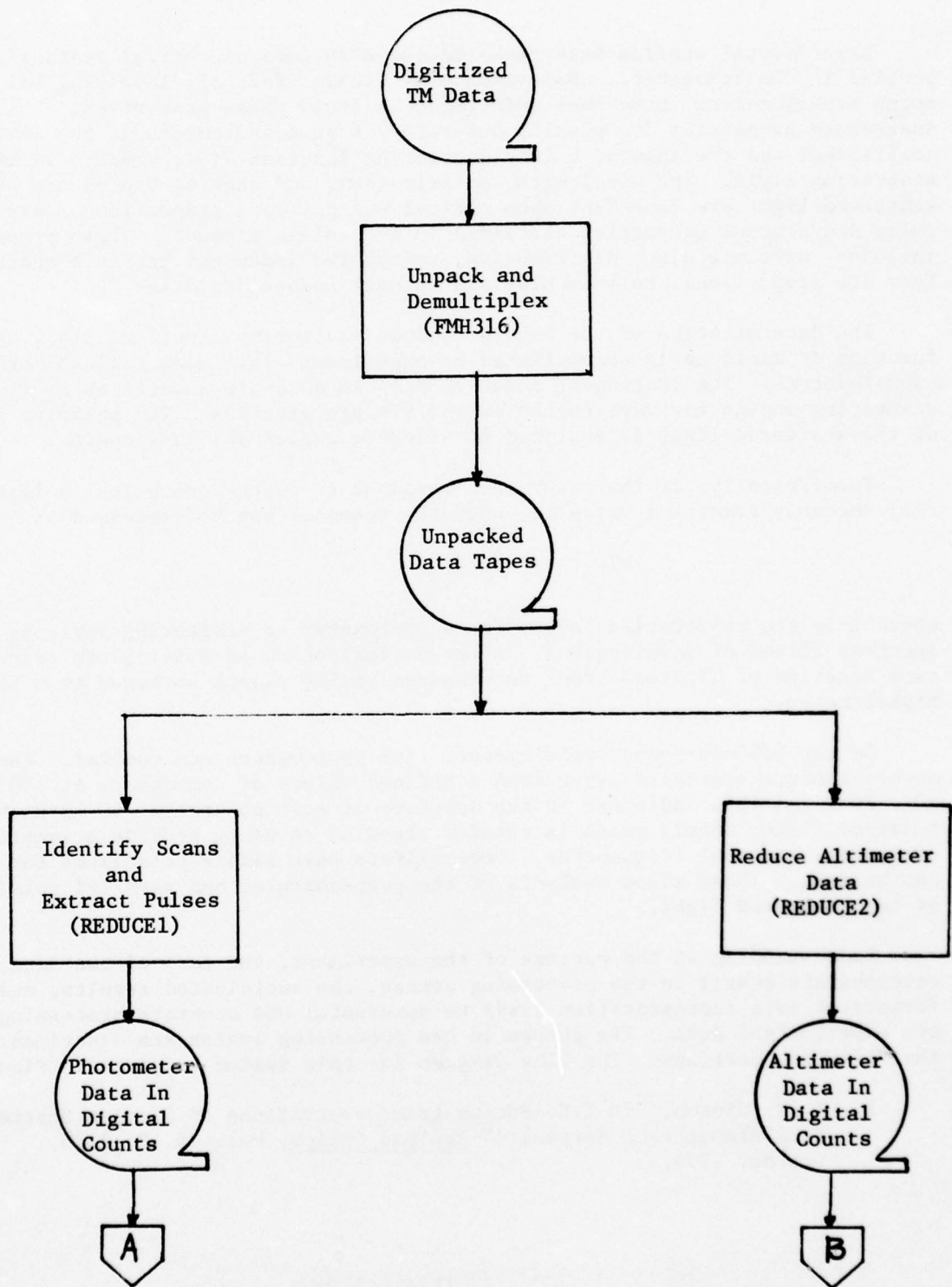


Figure 3.1 Nephelometer Data Processing System

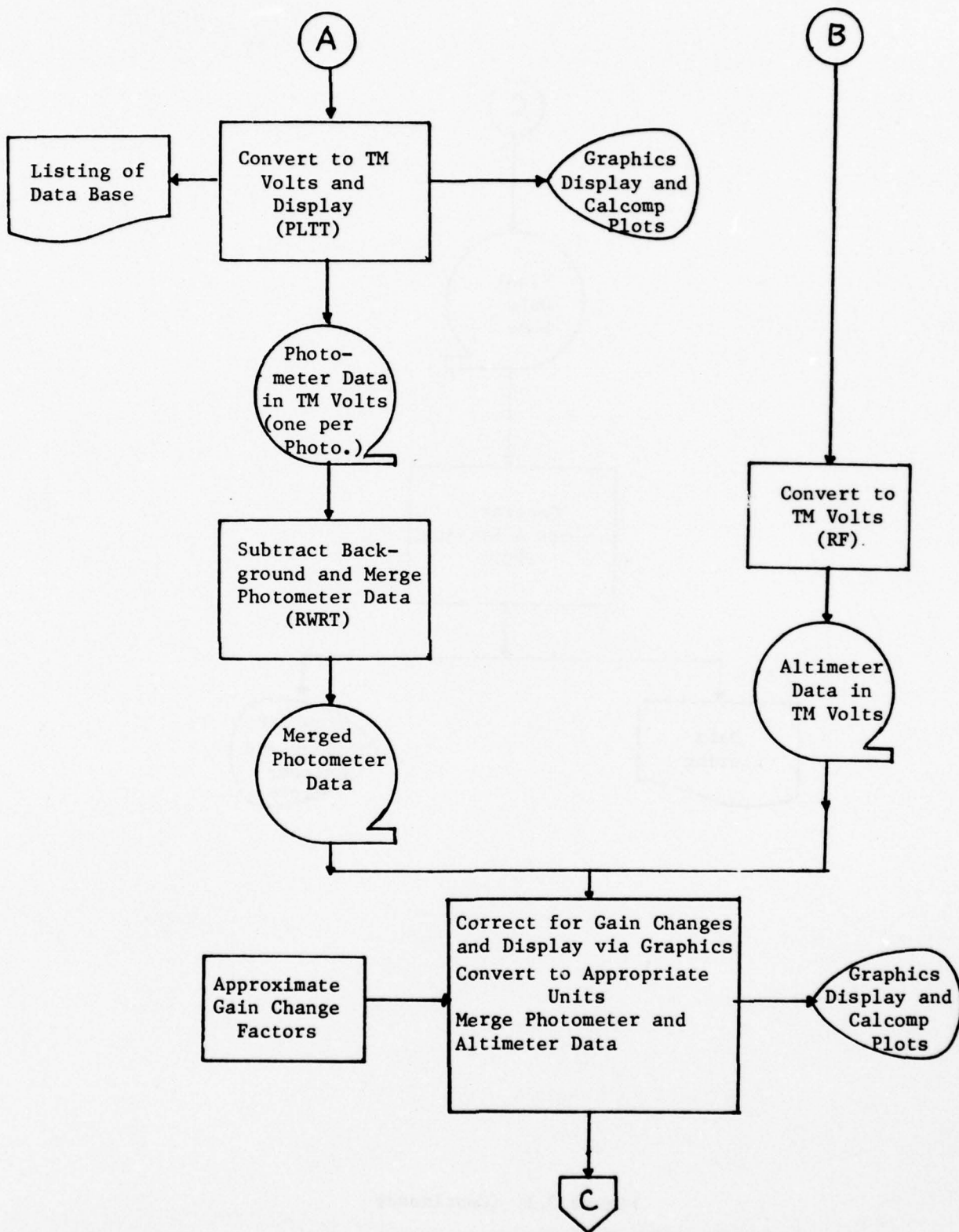


Figure 3.1 (Continued)

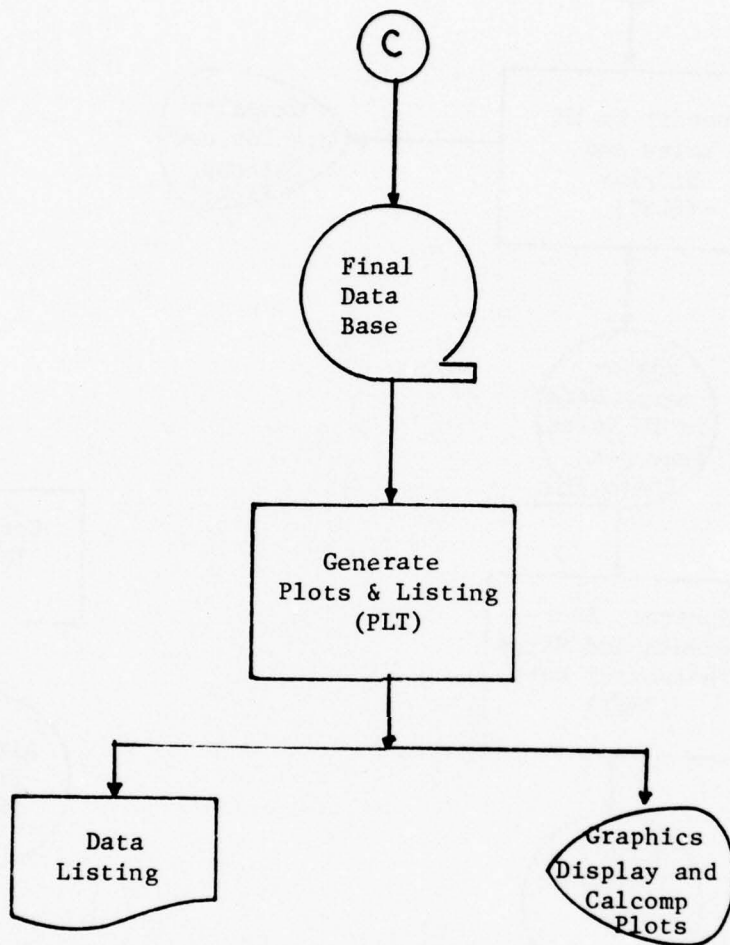


Figure 3.1 (Continued)

### 3.1 Data Reduction

#### 3.1.1 Preliminary

Many of the initial phases of the data processing are identical in function, if not detail, for the various types of balloon-borne experiments. The verification of the digital tapes and listing of the digitized counts are common to all experiments.

In this experiment, the analog signal voltages from the instruments are telemetered to a ground receiving station, where they are recorded on magnetic tape for computerized data reduction. A Honeywell H316 A/D System, installed at the Air Force Geophysics Laboratory Decommutation Center is used to convert the analog data to a standard digital format for analysis on a large scale digital computer. The format of these digital tapes is not directly compatible with the AFGL CDC 6600. Modular routines are used to unpack and convert the data to a format acceptable to the FORTRAN programs comprising this processing system.

Accompanying each digital tape is an analog to digital work request. It defines the contents and format of the digital tape to be processed. Each form contains the balloon flight identification, the type of digitization, time duration and channel source of each file. In the balloon-borne nephelometer experiment, the resulting data are from five photometers and one altimeter channel. The data samples are usually multiplexed during digitization, necessitating special processing before data reduction.

All digitized data tapes can be analyzed by program FMH316, which demultiplexes the data on the input tape and creates an output tape. The output tape is formatted to be acceptable as input to the analysis programs. FMH316 produces a summarized listing of the digitized counts versus elapsed time from launch and the time of occurrence. Usually, only selected portions of the data are listed. This printout (see Figure 3.2), in conjunction with an analog strip chart, is used to determine the minimum high calibrate and the maximum low calibrate for the conversion of the digital data to telemetry (TM) voltages.

#### 3.1.2 Pulse Identification and Reduce

Figure 3.3 illustrates a section of the stripchart used to display the analog data telemetered from the experiment package. The five traces at the top of this chart correspond to the outputs of the five photometers, and the last trace corresponds to the output of the altimeter. These six voltages are digitized and multiplexed together on a single reel of magnetic tape. Usually a digitization rate of 180 samples per second is used, which yields a rate of 30 samples per second for each of the six instruments. The method by which these traces are generated is described below.

An eight-position filter wheel is mounted in front of the entrance slit of each photometer. The filter wheel is rotated stepwise so as to provide a

722	17780.1	.20	17783.2	1.07	17786.2	.16	17789.3	2.73	17792.3
723	17804.6	.22	17807.6	.57	17810.7	.10	17813.7	2.75	17816.1
724	17829.0	.07	17832.0	.71	17835.1	.13	17838.1	2.76	17841.2
725	17853.4	.06	17856.5	.46	17859.5	.18	17862.6	2.60	17865.6
726	17877.8	.10	17880.9	1.15	17883.9	.05	17887.0	2.47	17890.1
727	17902.3	.27	17905.3	.90	17908.4	.09	17911.4	2.71	17914.5
728	17926.7	.07	17929.8	.66	17932.8	.13	17935.9	2.59	17938.9
729	17951.1	.35	17954.2	.70	17957.2	.08	17960.3	3.15	17963.3
730	17975.5	.26	17978.6	.59	17981.6	.25	17984.7	2.77	17987.7
731	17999.9	.08	18003.0	.83	18006.0	.34	18009.1	2.52	18012.1
732	18024.4	.09	18027.4	.64	18030.5	.09	18033.5	2.47	18036.6
733	18048.8	.34	18051.8	.78	18054.9	.26	18057.9	2.55	18061.0
734	18073.2	.19	18076.2	1.16	18079.3	.25	18082.3	2.14	18085.4
735	18097.6	.13	18100.6	.85	18103.7	.19	18106.7	2.36	18109.8
736	18122.0	.19	18125.0	.90	18128.1	.07	18131.1	2.60	18134.2
737	18146.4	.15	18149.4	.76	18152.5	.57	18155.6	2.61	18158.6
738	18170.8	.06	18173.9	.64	18160.2	.21	18180.0	2.38	18183.0
739	18195.2	.12	18198.3	.74	18201.3	.11	18204.4	2.93	18207.4
740	18219.6	.11	18222.7	.85	18225.7	.06	18228.8	2.26	18231.8
741	18244.0	.19	18247.1	.79	18250.1	.16	18253.2	2.10	18256.2
742	18268.4	.08	18271.5	.73	18274.5	.14	18277.6	2.46	18280.6
743	18292.9	.22	18295.9	1.01	18299.0	.27	18302.0	2.65	18305.1
744	18317.3	.33	18320.3	1.10	18319.2	.39	18320.4	2.30	18329.5
745	18341.7	.16	18344.8	.84	18347.8	.07	18350.9	2.84	18353.9
746	18366.1	.15	18369.2	.67	18372.3	.06	18375.3	2.32	18378.4
747	18390.6	.07	18393.6	.83	18396.7	.25	18399.7	2.52	18402.8
748	18415.0	.12	18418.1	1.19	18421.1	.06	18424.2	2.67	18427.2
749	18439.4	.15	18442.5	.68	18445.6	.31	18448.6	2.65	18451.7
750	18463.9	.06	18466.9	.95	18470.0	.19	18473.0	2.71	18476.1
751	18488.3	.15	18491.4	.94	18494.4	.19	18497.5	2.64	18500.5
752	18512.7	.18	18515.8	.81	18518.9	.04	18522.0	2.06	18525.0
753	18537.2	.18	18540.2	.79	18543.3	.07	18546.3	2.49	18549.4
754	18561.6	.08	18564.7	.61	18567.7	.10	18570.8	2.25	18573.9
755	18586.1	.15	18589.1	.74	18592.2	.15	18595.2	2.21	18598.3
756	18610.5	.10	18613.6	.87	18616.6	.26	18619.7	2.45	18622.8
757	18635.0	.09	18638.0	.49	18641.1	.10	18644.1	2.55	18647.2
758	18659.4	.09	18662.5	.81	18665.5	.19	18668.6	2.97	18671.6
759	18683.9	.17	18687.0	.53	18690.0	.05	18693.1	2.43	18696.1
760	18708.3	.12	18711.4	.88	18714.5	.15	18717.5	2.43	18720.6
761	18732.8	.34	18735.9	1.47	18738.9	.11	18742.0	2.41	18745.0
762	18757.3	.12	18760.3	1.35	18763.4	.11	18766.4	2.61	18769.5
763	18781.7	.11	18784.8	.88	18787.8	.24	18790.9	2.69	18793.9
764	18806.2	.19	18809.2	.79	18812.3	.25	18815.3	2.18	18818.4
765	18830.6	.34	18833.7	.81	18836.7	.08	18839.8	2.58	18842.8
766	18855.1	.06	18858.1	.56	18861.2	.05	18864.3	2.30	18867.3
767	18879.6	.05	18882.6	.97	18885.7	.29	18888.7	2.15	18891.6
768	18904.0	.07	18907.1	1.10	18901.8	.35	18913.2	2.52	18916.3
769	18928.5	.07	18931.6	.86	18934.7	.38	18937.7	2.60	18940.8
770	18953.1	.11	18956.1	.65	18959.2	.18	18962.2	2.42	18965.3
771	18977.6	.14	18980.6	.63	18983.7	.07	18986.7	2.16	18989.8
772	19002.0	.27	19005.1	.88	19008.2	.29	19011.2	1.84	19014.3
773	19026.5	.19	19029.6	.55	19032.6	.10	19035.7	2.41	19038.8
774	19051.0	.12	19054.1	.71	19040.5	.35	19060.2	2.42	19063.3

Figure 3.2 Printout of Digitized Nephelometer Data

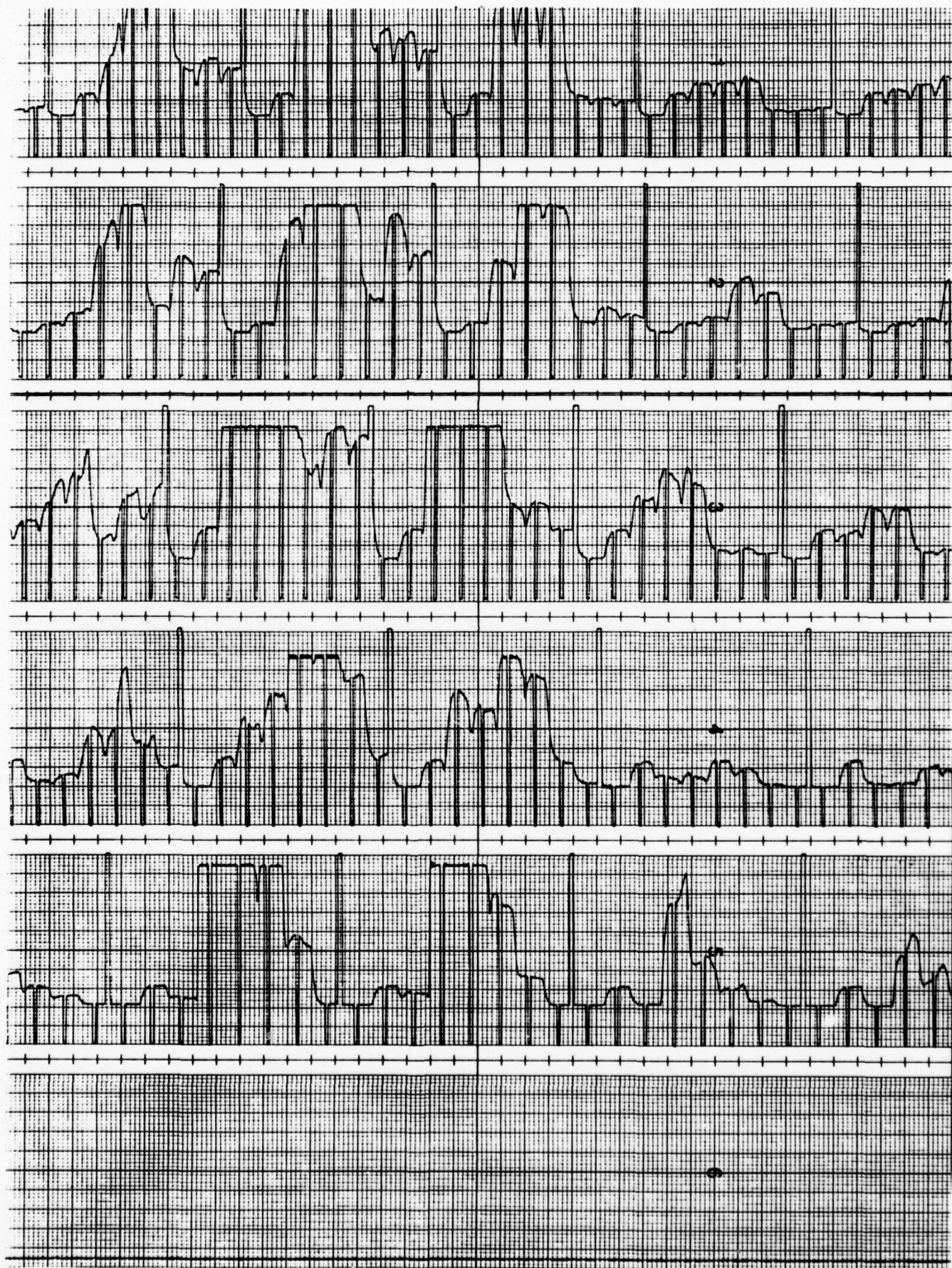


Figure 3.3 Nephelometer Data Stripchart

sampling rate of 3 seconds/filter. The midtime of each sampling interval is indicated by a -1.25 volt pulse, and the average of the voltage for a short time before and after this pulse constitutes the datum at that time. The start of a filter wheel scan is indicated by a 5 volt synchronization pulse. Thus the outputs of the photometer channels consist of a series of pulses, every three seconds; a 5 volt pulse followed by eight -1.25 volt pulses, with the voltages in between pulses being proportional to the photometer reading at one of the eight filter positions.

Program REDUCE1 searches for experimental scans having eight pulses occurring sequentially. The start of a scan is identified first. The start occurs when an area has been found containing several data greater than a specific value, PULHI, determined during the preliminary data review. The average, as a 5 volt indicator, is then computed. Eight areas must follow having few data lower than a certain value, PULLO, and the average, as a -1.25 volt indicator, is computed. The midpoint of each pulse from the -1.25 volt indicator must be determined. The four points on either side of the indicator, corresponding to when the signal is dropping or rising, are ignored. Twenty points per indicator, ten preceding and ten following the indicator, contribute to the data base. Scans are eliminated if their pulses do not conform to the above criteria, or there are not eight -1.25 volt pulses in succession. When a data scan is found to be in error, it is so noted in the listing. The bad scan listing usually will reveal problem areas in the flight.

A file is created consisting of the time, average HI calibration, average LO calibration, and the twenty points for each filter in a scan.

### 3.1.3 Data Conversion and Display

The next phase in the processing system is the conversion of the data on the digital tapes to telemetry volts. This is a simple linear conversion using the high and low calibrates, determined above. The range of the TM voltages in this experiment is from -1.25 to 5 volts, corresponding to the peaks of the synchronization pulses described earlier. The data on the digital tape range from -2048 to 2048 "digital counts". The average minimum and maximum digital counts (determined earlier by REDUCE1) correspond to -1.25 and 5 TM volts, respectively. The intermediate voltages are determined linearly, using these numbers as calibrates.

This conversion is accomplished by program PLTT. It also reads the reduced data file and averages the 20 data points saved for each pulse. After the average voltage in each pulse is determined, there will be only one data point for each pulse to be saved. There are eight pulses for each rotation of the eight-position filter wheel in each photometer.

The data base consists of voltages vs. elapsed time. For each rotation of the filter wheel, a record is written containing the eight sets of data, i.e. the average of the 20 points associated with each pulse. This data base is written

to a system permanent file, using the random access routines, for convenience in further processing.

PLTT also allows the user to display the data voltages, as a function of elapsed time, on the interactive graphics console screen for a preliminary view. The user is then able to ascertain whether data reduction has been successfully accomplished. In addition, Calcomp plots of voltages vs. elapsed time of each pulse for each photometer can be generated. The identification of the experiment events (pulses) also associates the event with an elapsed time from launch. Plots and listings of this association usually are sufficient for pulse identification verification purposes.

#### 3.1.4 Altitude Determination

The balloon's altitude is used as a common frame of reference. Later ascent and descent portions of the experiment results are often compared for self-consistency. The altitude of the experiment package is determined both by transponder tracking systems and by an on-board altimeter. The altimeter data is telemetered to the ground, where it is recorded along with the instrument data. Program REDUCE2 is used to unpack and demultiplex this data.

The altitude parameter is determined from reduced altimeter data with elapsed time from launch as the independent variable. Since the altimeter data is recorded as digital counts, it first has to be converted to telemetry voltages, using a linear calibration. The range of this voltage is from 0 to 5 volts. Program RF is used to create a permanent file containing altimeter data in TM volts with elapsed time from launch. Later, when the altimeter has been calibrated, these TM voltages are converted to altitude in kilometers, using a linear calibration supplied by the researcher.

#### 3.1.5 Background Corrections

The first of the eight filters on each filter wheel is opaque to the radiation impinging on the photometer. The signal measured when this filter is in position is the background signal (due to noise, randomly scattered radiation, etc.) to be subtracted from the signal measured when the remaining six filters are in position. Thus the background signal for each photometer is sampled once every rotation of the filter wheel.

Consequently the first datum in each eight-filter scan represents the background signal by which the following seven data are augmented. Program RWRT performs this correction and creates a data file with six background-corrected data points per filter scan. (The data from one of the filters is not used by this processing system.) This data file is created using the random access routines in order to facilitate the remaining processing.

## 3.2 Conversion of Telemetry Voltages to the Measured Parameters

### 3.2.1 Gain Change Corrections

Several mid-flight gain changes were made, enabling signals to be received over several orders of magnitude below those observed at ground level. As the experiment package ascends through a less dense atmosphere, the sensitivity of the instruments on board must be increased to compensate for the reduced signal received. These gain changes are made remotely, by the researcher on the ground, while monitoring the telemetered signals. Consequently, the outputs of the photometers, rather than being monotonically decreasing with increasing altitude, exhibit jumps in the signals at the times at which the gain changes were made (see Figure 3.4). Before these data are of any use, they must be corrected for these gain changes.

These gain changes increase or decrease the instrument sensitivity by a constant factor. To correct the data, one must determine the times of the gain changes and the factors by which the instrument sensitivities were changed. Then the data in between gain changes is adjusted by the gain change factors in the appropriate regions to yield a data base in which all the voltages are with respect to the ground level observation.

An interactive graphics program, SPLOT, has been developed to facilitate these gain-change corrections. This program displays the voltage versus elapsed time data on the graphics screen and permits the researcher to observe the effects of changing the gain change factors. The times of the gain changes are determined by examining the listings of the raw data, which were generated earlier. The researcher and analyst observe the data profiles for each filter of each photometer and determine the gain change factors to be used. This program creates an output file consisting of corrected voltage versus elapsed time data for each profile. Additionally, hard copy (pen and ink) plots of the final data bases are also generated by this program.

### 3.2.2 Conversion to the Measured Parameters

The next phase after the gain change corrections to the telemetry voltages is converting the data to the units of the measured parameters (photometer intensities). Each photometer is calibrated prior to flight and postflight. Variations in the lenses, filters, etc., are constants accounted for in the instruments calibration factors. This calibration factor is supplied by the researcher after experimental determination, and is multiplied by the corrected voltages, to obtain the measured parameter.

The balloon height profile is generated by connecting time to altitude heights from the altimeter data and provided calibration. The data base containing the volume scattering function ( $KM^{-1}-SR^{-1}$ ), altitude (KM), and total number of data points for each instrument or scattering angle are generated onto a system random access file for further processing.

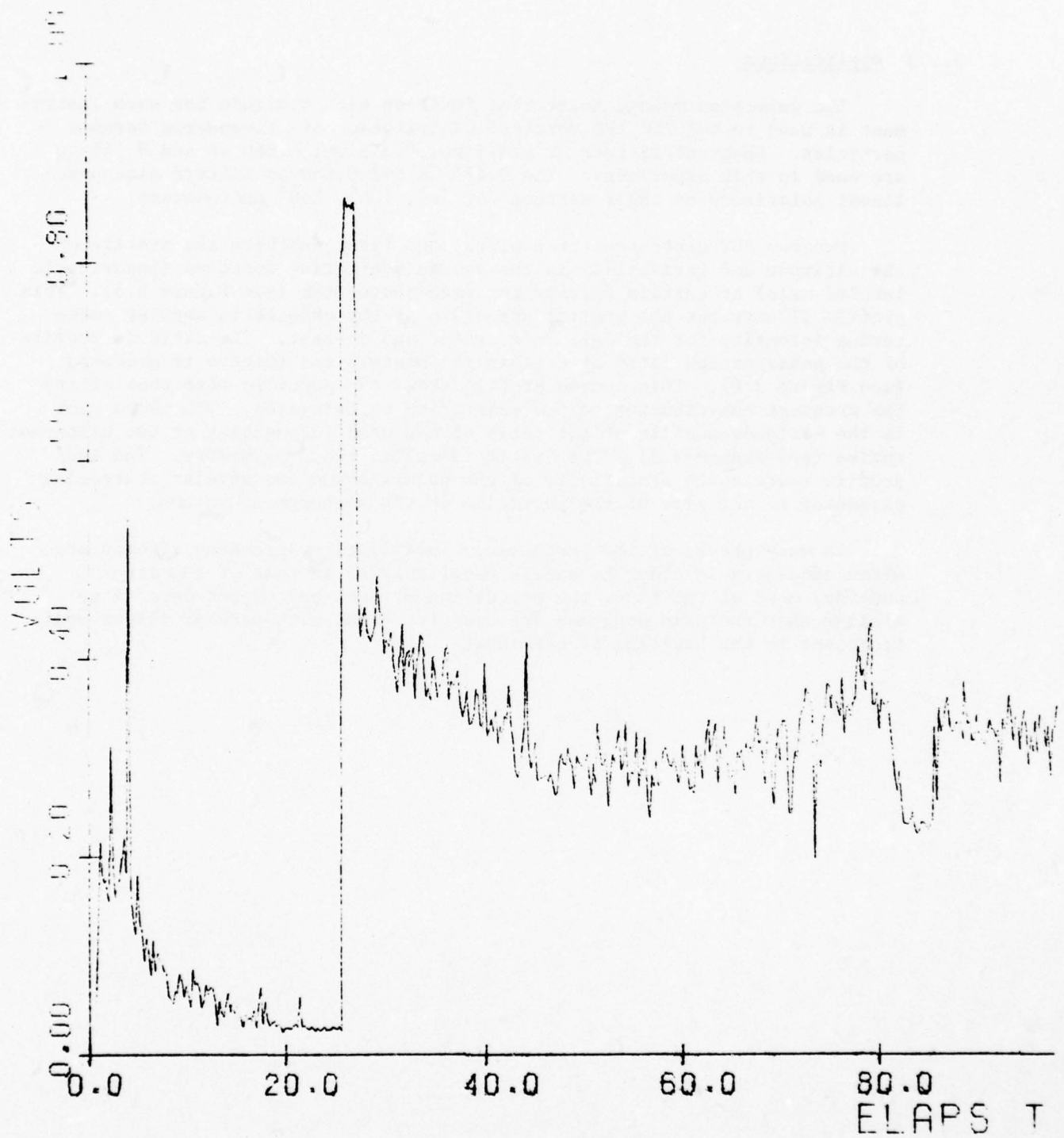


Figure 3.4 Nephelometer Data Profile Illustrating Gain Change

### 3.2.3 Applications

The generated volume scattering function with altitude for each instrument is used to analyze the vertical distribution of atmospheric aerosol particles. Spectral filters at 0.475  $\mu\text{m}$ , 0.515  $\mu\text{m}$ , 0.660  $\mu\text{m}$  and 0.745  $\mu\text{m}$  are used in this experiment. The 0.475  $\mu\text{m}$  and 0.660  $\mu\text{m}$  filters also have linear polarizers on their surface for 50°, 100°, 150° photometers.

Program PLT generates three plots; the first exhibits the profile of the altitude and variability in the volume scattering function (logarithmic labeled axis) at certain filters for each photometer (see Figure 3.5). This profile illustrates the general structure of the changes in angular scattering intensity for the balloon's ascent and descent. The altitude profile of the polarization ratio of certain photometers and filters is produced (see Figure 3.6). This second profile shows the particle size that offers the greatest contribution to the scattering polarization. The third plot is the altitude profile of the ratio of measured intensities at two different angles (see Figure 3.7). This ratio is called the dissymmetry. The last profile reveals the sensitivity of the polarization and angular scattering parameter to the size of the particles in the measurement volume.

In many phases of the processing, individual programming efforts are often necessary in order to handle peculiarities in some of the data. However, most of the time, the processing of each photometer data is so similar that the same programs are used for each, with perhaps slight modifications in the handling of the input.

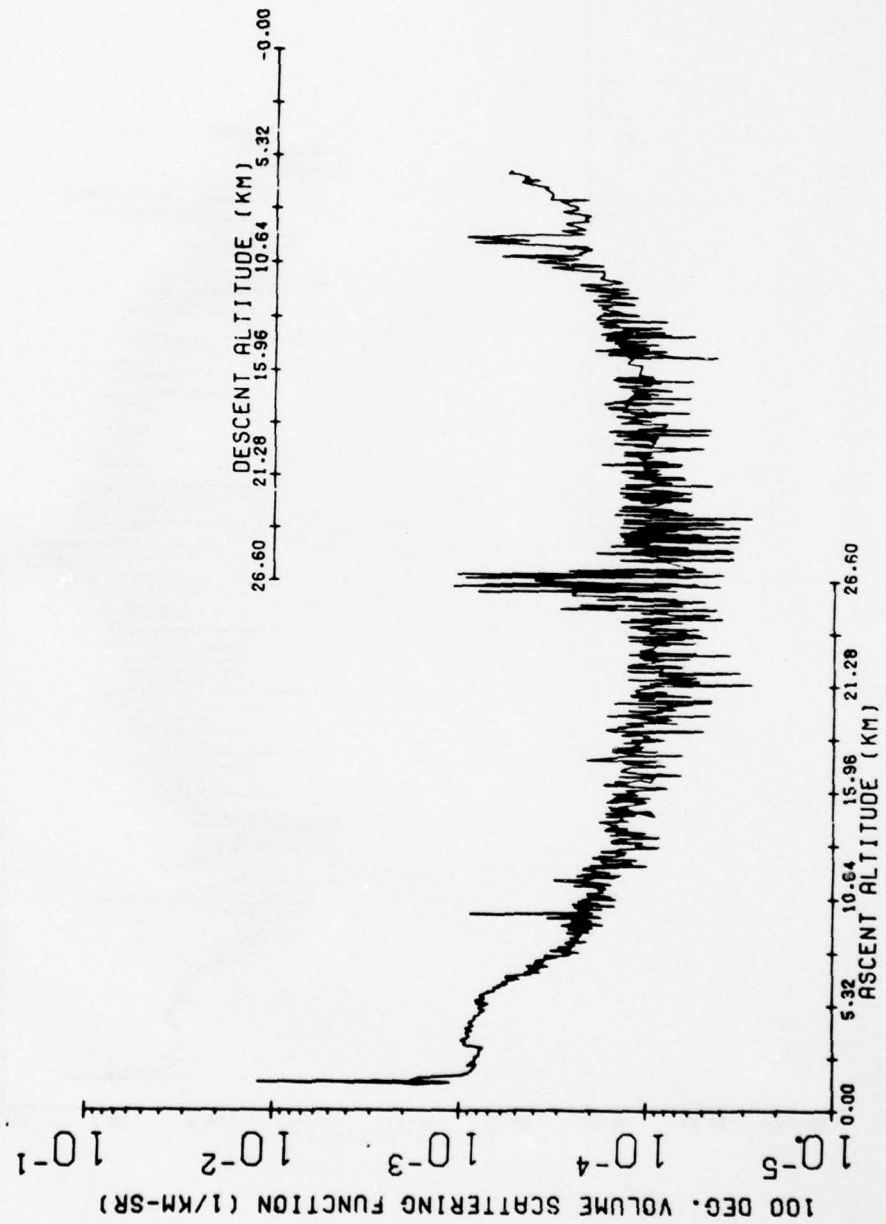


Figure 3.5

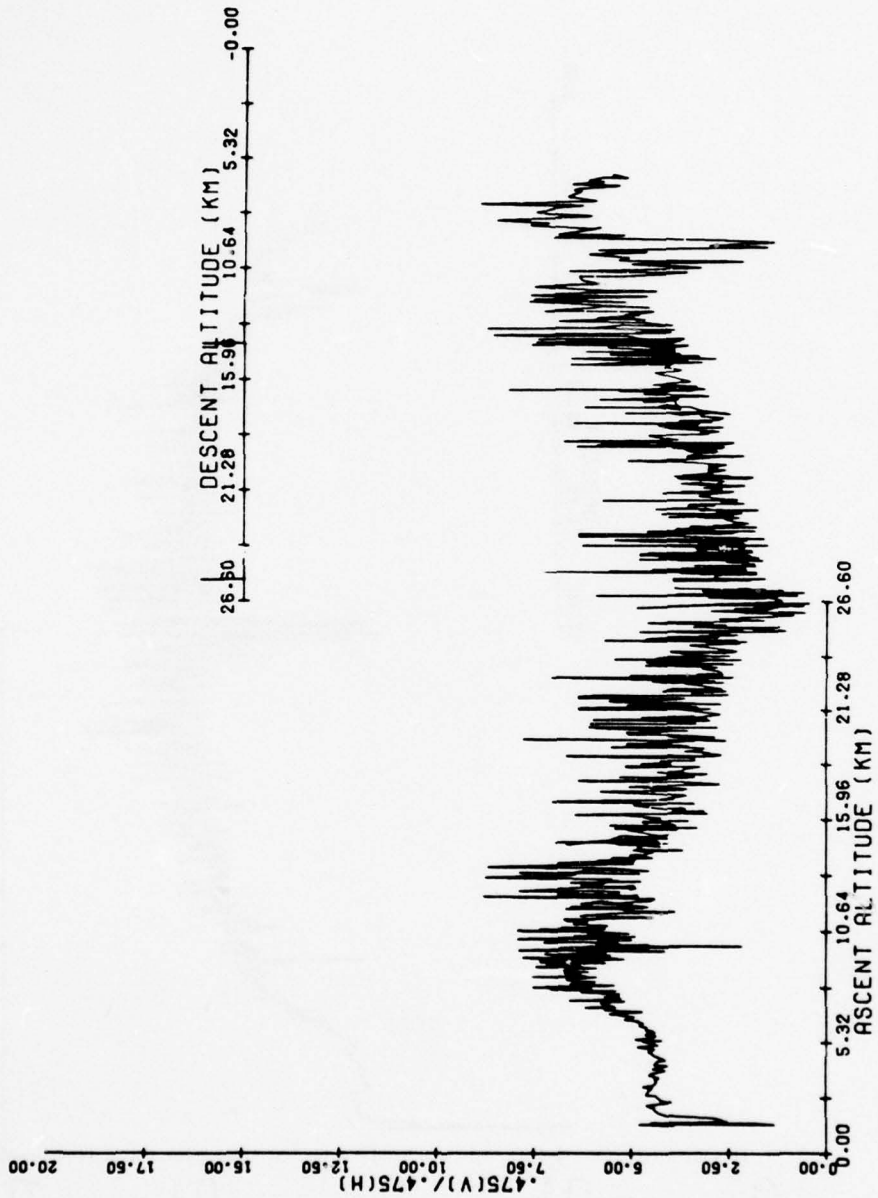
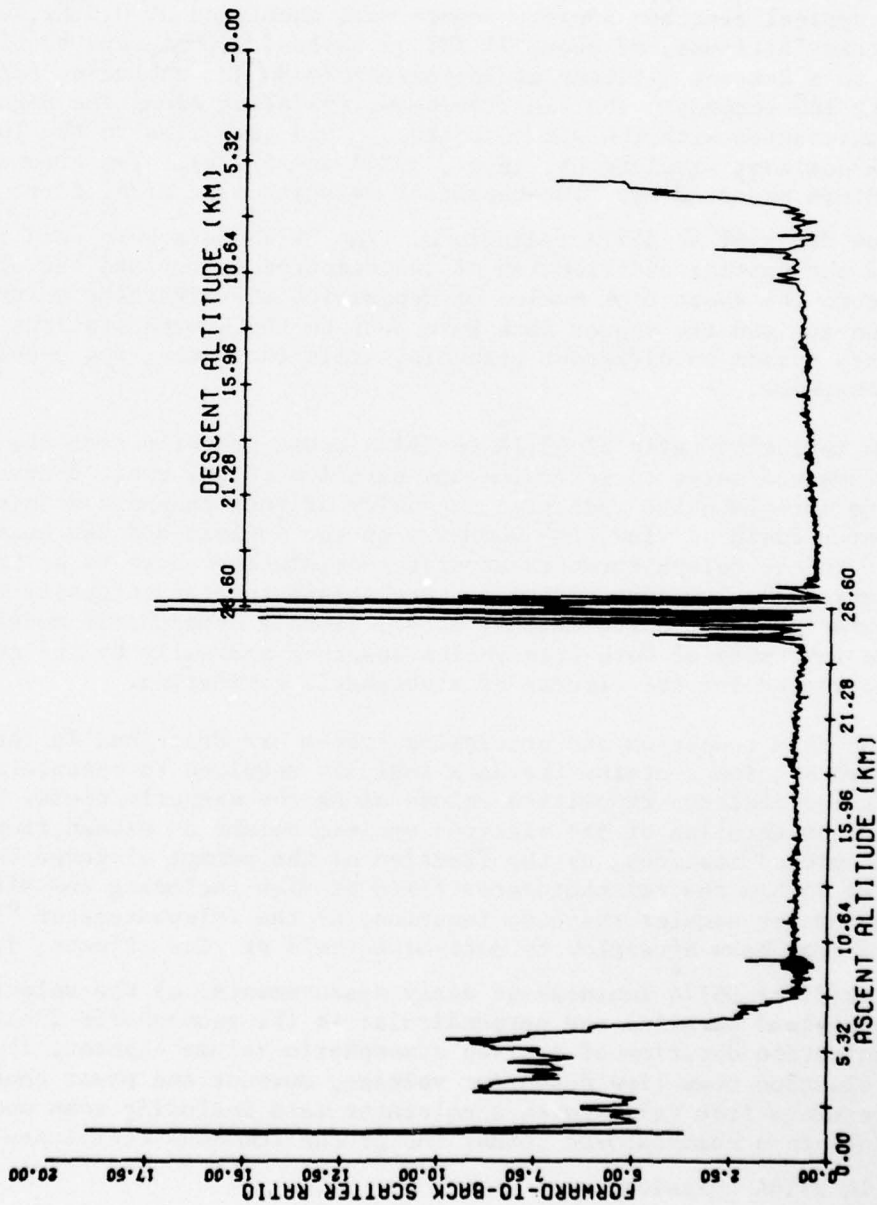


Figure 3.6



FORWARD-TO-BACK SCATTER RATIO AT .475(V) MICRON VS ALTITUDE

Figure 3.7

#### 4.0 A PROCESSING SYSTEM FOR ROCKET-BORNE ELECTRON ACCELERATOR EXPERIMENT DATA

Rocket-borne experiments, coordinating an Electron Accelerator, and a number of optical and infrared sensors, were performed to measure the distribution of the electron energy deposition in the atmosphere, and to detect the electro-magnetic radiations induced by the electrons.

A typical electron source, square wave modulated at 0.5 Hz, was initiated at a rocket altitude, of about 75 KM, on payload ascent, and continued through apogee to a descent altitude of approximately 80 KM, operating for an interval of about 180 seconds. The electron beam, spiraling along the magnetic field lines interacted with the air constituents and gave rise to the luminences at several dominant wavelengths, (e.g., 3914Å and 5577Å). Two ground based telephotometers measured the time-dependent emission rate of  $N_2^+$  first negative 3914Å and slow decay  $0(1s)$  5577Å radiations. The 3914Å data were used for the measurement of the spatial distribution of the electron energy and the 5577Å data served to measure the short time motion of deposition and afterglow volume. All the electron gun and the sensor data were sent to the ground stations through the telemetry system on different channels, while the rocket was passing through the atmosphere.

An intensity ratio of 5577Å to 3914Å could properly test the interaction mechanisms and serve to determine the duration of the excited atmosphere. In order to integrate the radiation intensity of both channels within the telephotometer field of view, the geometry of the payload and the beam length with respect to the telephotometers at different stations have to be known before calculating the luminous efficiency and telephotometer intensity ratio. During the course of these calculations, a 1971 Jacchia atmospheric model was utilized and the intensity of both frequencies absorbed partially by the atmosphere were also corrected for the effects of atmospheric extinction.

The data reduction and processing system are described in the next section. The third section contains the data analysis required to calculate: a) The size of the electron deposition volume along the magnetic field, b) the apparent size and orientation of the electron excited volume as viewed from the different optical ground stations, c) the fraction of the prompt electron beam luminescence observed within the telephotometer field of view including the effects of the telephotometer angular response function, d) the telephotometer "look time" in the electron beam afterglow to determine field of view effects, if any, on the slow  $0(1s)$  5577Å luminescent decay measurements, e) the velocity components of the payload parallel and perpendicular to the geomagnetic field to determine the excitation duration of a given atmospheric volume element, f) the rocket-borne electron beam time dependent voltage, current and power characteristics as determined from telemetered accelerator data including some monitors available only in a commutated format and g) the luminous efficiency for production of  $N_2^+$  1N 3914Å emissions.

The overall flowchart of the linking among the data reduction and/or processing and analysis is presented in Figure 4.1.

#### 4.1 Data Reduction

Rocket-borne experiment data are telemetered to the ground stations through the different telemetry channels. The outputs of these experiments, for instance, the electron gun data, are transmitted by the FM/FM carrier system which permits the simultaneous transmission of the outputs of multiple detectors. The outputs are recorded on magnetic tape in analog form at the site of launching, and later are digitized by the Honeywell H-316 analog to digital system.

For the electron accelerator experiments, there are electron gun (accelerator) data, and telephotometer data involved in the calculation of luminous efficiency and telephotometer intensity ratio. Data reduction of both types of data are described in the following two subsections. An additional topic, concerning the determination of the gun pulse on-off times, is also presented in the third subsection.

##### 4.1.1 Electron Gun Data

The electron gun data consists of the voltages and currents of each of three guns and are telemetered through both the commutator (FM/FM/PAM) and continuous (FM/FM) channels. All the voltages are telemetered on commutator channels and all the currents on continuous channels. In addition, the gun 1 voltage data is also linked through a continuous channel to serve as an additional check on the electron gun system. The commutator has 64 sequences per frame and samples at a rate of 2.5 frames per second. The gun voltage and current data are linked through six commutator sequences, hence the absolute value of gun power is measured over a time slip of 37.5 ms.

The data to be processed, both from the commutator and the continuous channels, are provided in digital form and have to be converted to the appropriate units. For example, the electron gun data are to be converted to the units of volts and amperes. First the data are converted from "digital counts" to telemetry (TM) voltages, which usually range from 0 to 5 volts. Then the data are converted to the units of the measured parameter, using calibration constants provided by the experimenter.

Prior to launch, a staircase potential is generated through the telemetry system (see Figure 4.2). Signals at 0, 1, 2, 3, 4 and 5 volts, for 1 second durations are generated for calibration purposes. Later when the data are digitized, the voltages at each of these steps are associated with the corresponding digital count on the tape. A linear fit is performed to determine the constants to convert the digital counts to telemetry volts.

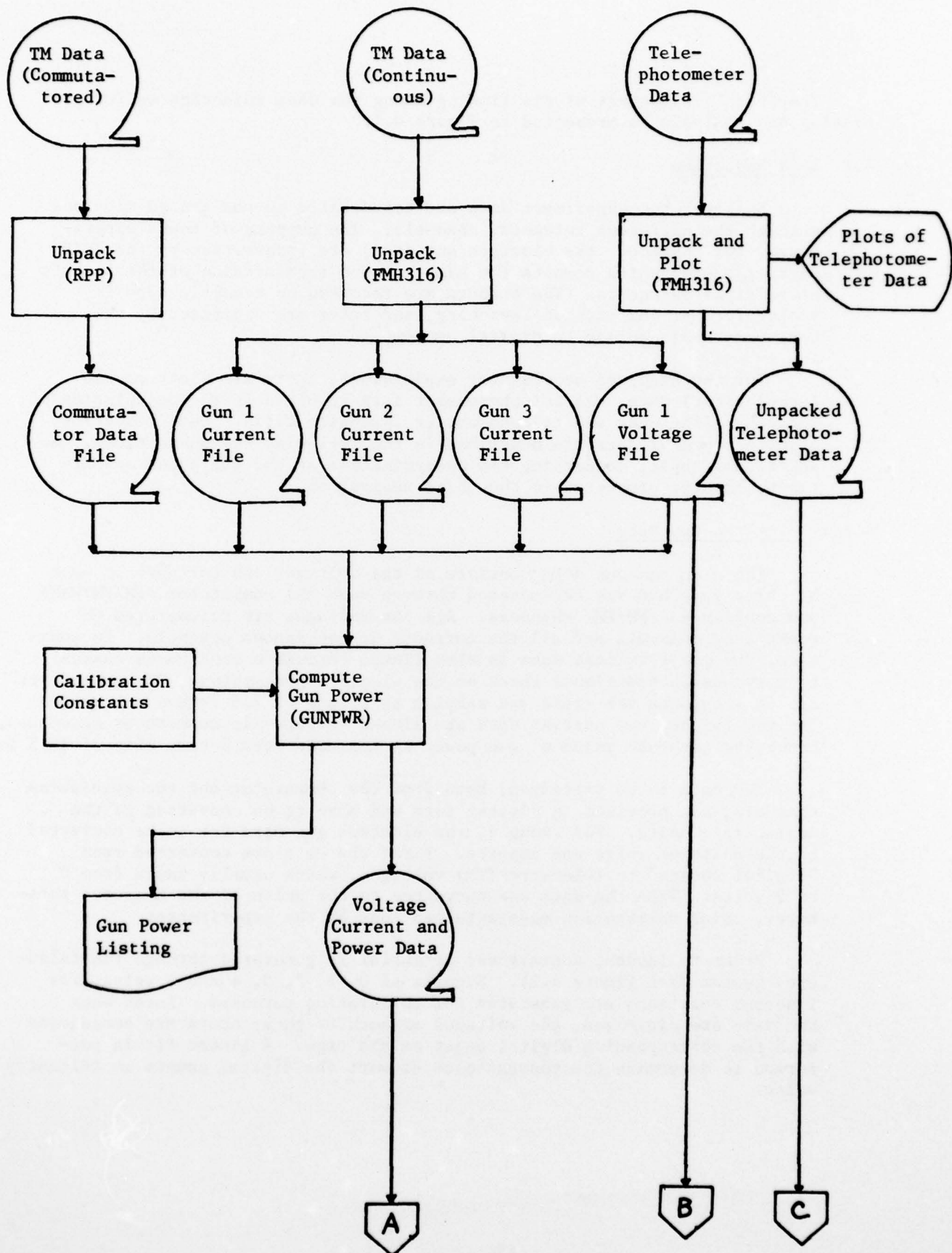


Figure 4.1 Flow Diagram of the Processing System For The Electron Accelerator Experiment Data

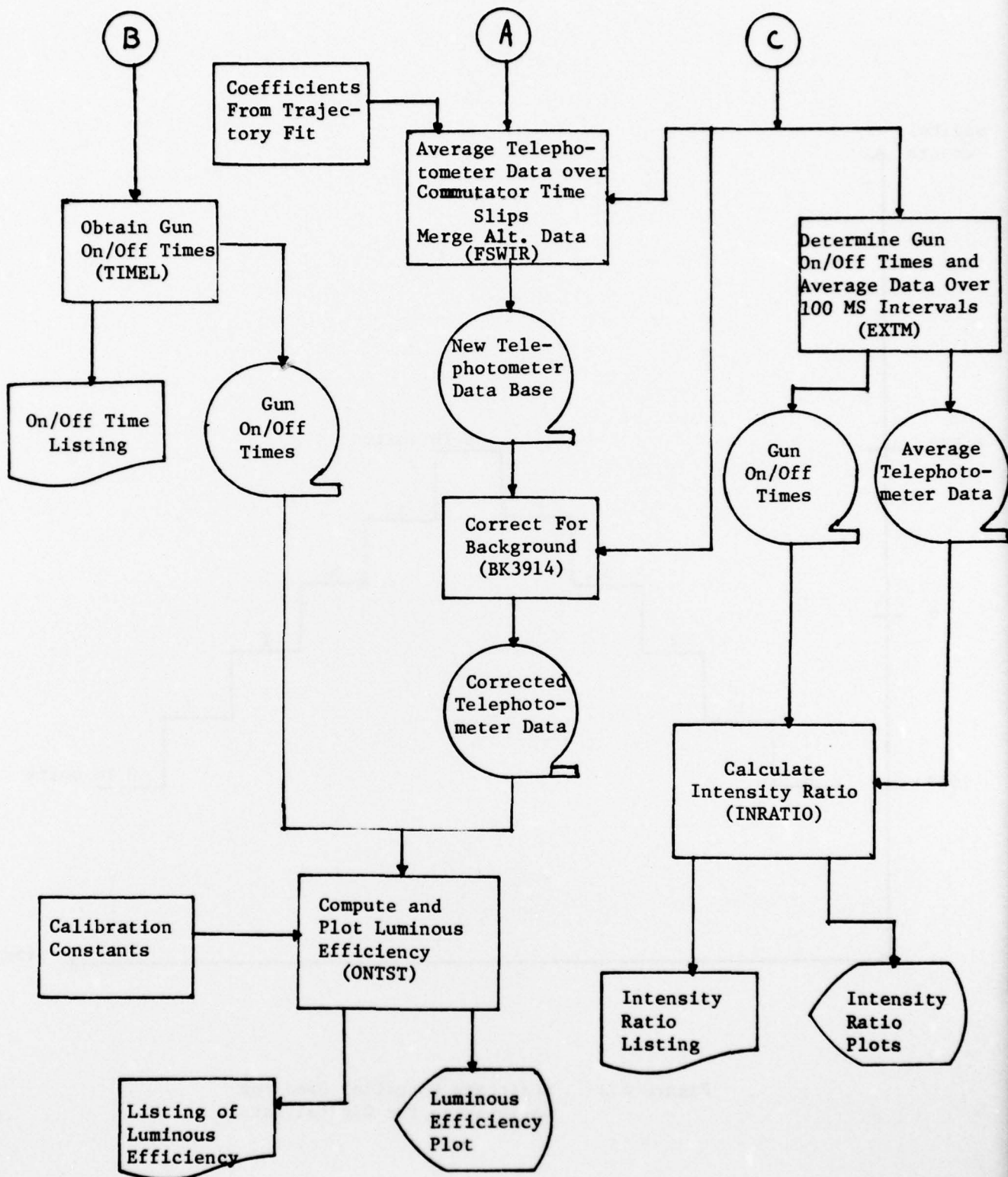


Figure 4.1 (Continued)

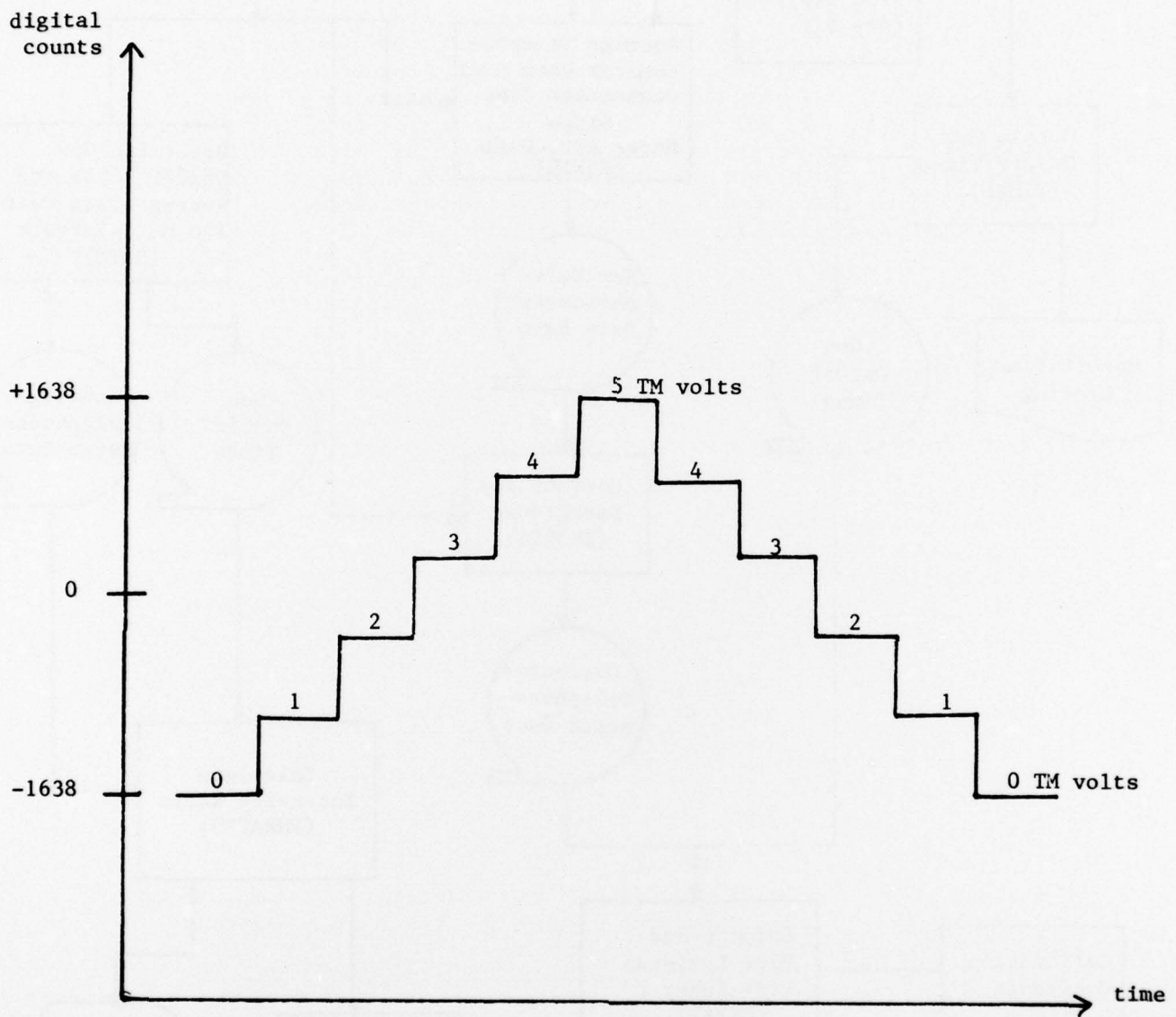


Figure 4.2 Staircase Potential Used for Calibrating the Digital Data

The data processing begins with copying the original magnetic tapes which contain the digital data, to computer center tapes. The original tapes are then kept for backups. Since the packed data formats used on these tapes are incompatible with the CDC 6600, modular routines are used to read, unpack and convert the data to a format which can be used by the FORTRAN programs which comprise this processing system. The commutator data is processed through the standard "Rocket Processing Package" (RPP) to create the commutator data base. Program FMH316 is used to process the data from the continuous channels. RPP could be used to process the continuous data also, but the shorter and faster FMH316 program is usually more convenient.

These two data bases are used by program GUNPWR to calculate the total gun power, that is, the total energy deposited in the atmosphere at each pulse of the guns. The power of each individual gun is simply the product of the gun current (obtained from the continuous channel data) and the gun voltage (obtained from the commutator data). The total gun power is also computed. This computation is made once for each sweep of the commutator, at times corresponding to when the commutator is sampling the voltage of the particular gun. This provides 2 to 3 points per gun pulse. Additionally, the gun 1 voltage data, obtained from the continuous channel, is averaged over the same time interval as when the commutator is sampling the quantity. This average is noted in the listing for comparison purposes. A data base is created which contains gun pulse number, time, voltage, currents and power for each of the three guns and the total power.

The file contains one record for each sweep of the commutator. The contents of each 15 word record are described below:

- Word #1 = Pulse number
- #2 = Elapsed time at the center of each commutator group (sec)
- #3 = Continuous gun 1 voltage averaged over the time the commutator is sampling the gun 1 voltage (KVolt)
- #4 = Commutated gun 1 voltage (KVolt)
- #5 = Gun 1 current (Ampere)
- #6 = Gun 1 power (KWatt)
- #7 = Continuous gun 2 voltage averaged over the time the commutator is sampling the gun 2 voltage (KVolt)
- #8 = Commutated gun 2 voltage (KVolt)
- #9 = Gun 2 current (Ampere)

- Word #10 = Gun 2 power (KWatt)
- #11 = Continuous gun 3 voltage averaged over the time the commutator is sampling the gun 3 voltage (KVolt)
- #12 = Commutated gun 3 voltage (KVolt)
- #13 = Gun 3 current (Ampere)
- #14 = Gun 3 power (KWatt)
- #15 = Total power of all three guns (KWatt)

This data base is retained as a system permanent file during the processing, and later is used in the computation of the luminous efficiency.

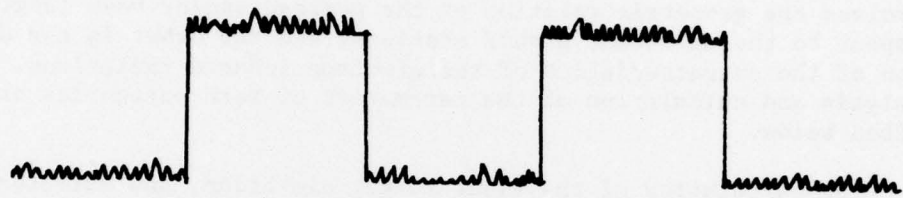
#### 4.1.2 Telephotometer Data Processing

Two ground-based telephotometers recorded the intensities of the induced emissions at wavelengths of 3914Å and 5577Å respectively. The data were recorded on magnetic tape and were later digitized in the same manner as telemetry data.

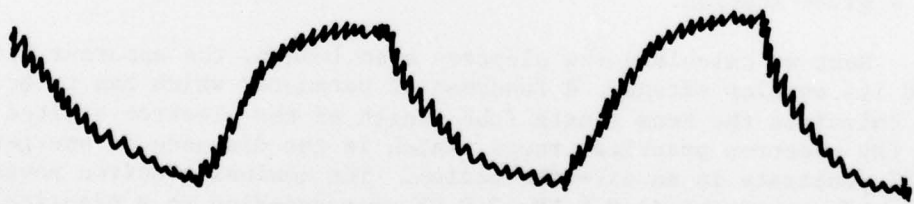
In order to verify and obtain a noise free data base, raw data plots are generated for each telephotometer by plotting the intensity (in digital counts) versus elapsed time. This raw data display assists the analyst in locating the noisy data; later it can be smoothed and edited if necessary. A list of the raw data is also available for the correction and identification of the sudden change of time dependent background level. Representative plots of both 5577Å and 3914Å intensity data are shown in Figure 4.3. Note that the 3914Å data shows the characteristics of square wave pulses and the 5577Å data of exponential growth and decay as a function of elapsed time.

#### 4.1.3 Determination of the Electron Gun Pulse On-Off Times

The electron gun accelerated the electrons along the magnetic field lines at an on-off frequency of 0.5 Hz. Since both 3914Å and 5577Å radiations are induced by the electrons interacting with the atmosphere, the determination of the gun pulse on-off times is necessary for the calculations of the luminous efficiency and telephotometer intensity ratio. Both the telephotometer data and continuous (gun 1) voltage data are used to determine the gun on-off times by setting a threshold level, above which the gun is considered to be "on". For example, a level of 1 TM volt, (corresponding to 343.5 digital counts) and of 0.150 KV, (corresponding to -1557 digital counts) are taken as the criteria for the data of 3914Å emissions and of the continuous (gun 1) voltage channel respectively, for the EXCEDE:SWIR experiment data.



(a) 3914Å data



(b) 5577Å data

Figure 4.3 Time Dependent Telephotometer Data

Program EXTM determines the gun on-off times on the basis of the 3914A telephotometer data. It creates a data base of gun on-off times for use as input to the calculation of the luminous efficiencies. Program TIML performs the same analysis, but using the electron gun voltage data. The on-off times determined by EXTM are also used as input to the program which calculates the telephotometer intensity ratios.

#### 4.2 Data Analysis

Our part of the analysis of the data from the rocket-borne electron accelerator experiments falls into two general categories. The first involves the geometric relation of the payload and/or beam length with respect to the different ground stations, and the other is the determination of the characteristics of the electron induced radiations. The analysis and calculation of the parameters of both categories are described below.

The calculation of the slant range, elevation, and azimuthal angle are done by the ONTST program using the following equations:

$$SL = \sqrt{(X-XS)^2 + (Y-YS)^2 + (Z-ZS)^2}$$

$$\phi = \tan^{-1} \left( \frac{Y-YS}{X-XS} \right)$$

$$\theta = \sin^{-1} \left( \frac{Z-Zs}{SL} \right)$$

Where SL,  $\phi$ , and  $\theta$  are slant range, azimuthal and elevation angle respectively.

X, Y, Z is the location of the payload and Xs, Ys, Zs is the position of a given station.

Next we calculate the electron beam length, the apparent beam length and its angular extent. A fundamental parameter which has to be known to calculate the beam length (the length of the electron excited column) is the electron practical range, which is the distance an energetic electron will penetrate in an air-like medium. The nominal electron power for this type of experiment is 2.5 KV ~ 3.0 KV corresponding to a practical electron range of  $2.2 \times 10^{-5} \sim 2.97 \times 10^{-5} \text{ gm/cm}^2$ . It is used along with the 1971 atmospheric Jacchia model to determine the electron beam length. The use of the atmosphere model is subject to the range of altitude of interest, for instance, the use of this Jacchia model is good for the altitude range of 90 KM to 130 KM.

The logarithm of the total density,  $\rho(z)$ , from the Jacchia model, for the time of the launch is fitted with piecewise polynomials, from 90 KM to 130 KM. These polynomials are then incorporated into a subroutine that

can rapidly compute the integrated vertical column density,

$$\int_{z_0}^z \rho(z) dz.$$

The beam length at an altitude  $z_0$  is then computed. The beam length,  $z_1 - z_0$  is found by solving for  $z_1$  in the equation:

$$\int_{z_0}^{z_1} \rho dz = P \sin \phi$$

where  $P$  is the practical electron range and  $\phi$  is the angle between the magnetic field and the horizontal plane.

Next the apparent lengths and orientations of the electron beam as viewed from the ground stations are computed. The following geometric configuration is defined before we go on to carry out the computation.

Let a viewing device  $V$  (telephotometer or camera) be located at the origin of a coordinate system, and let the tracking vector,  $\bar{R}(T)$ , be a vector with initial point at the origin and terminal point at the rocket. Also, let the beam vector,  $\bar{B}(T)$ , be a vector with initial point at the rocket and terminal point at the beam tip. Further, let  $\bar{N}(T)$  be a vector which lies along the line of sight of  $V$  and which points in the direction of vision. Finally, let  $P$  be the plane which passes through the rocket's position and which is perpendicular to  $\bar{N}(T)$ , and denote the projection of a vector  $A$  on  $P$  by  $A_p$ .

Since  $V$  sees only the projection of the beam on  $P$ , we define the apparent beam length,  $APBL$ , to be  $\bar{B}_p(T)$ .

The apparent vertical angle,  $APVANG$ , we define to be the angle between  $\bar{K}_p$  and  $\bar{B}_p(T)$ .  $\bar{K}$  is the unit vector in the direction of the positive vertical. From the point of view of a photograph,  $APVANG$  is the angle between the image of  $\bar{B}(T)$  and a vector pointing up which is parallel to the vertical edge of the photograph. Here we are assuming that the camera is not tilted in the sense that a vertical object has an image which is parallel to the vertical edge of the photograph.

Also,  $APHANG$ , the apparent horizontal angle is defined so that in the case of an untilted camera, it equals the angle between the image of the beam and the horizontal edge of the photograph. To remove the ambiguity, we precisely define it as the angle between  $\bar{B}_p(T)$  and a vector parallel to the bottom edge of the photograph having a positive  $X$  component.

$\bar{B}(T)$  was determined by the beam length and magnetic field direction, while  $\bar{N}(T)$  was taken to be the line of sight of the telephotometer, which was 1 miliradian below the payload.

The dot product was used heavily in the computation of the necessary projections; the projection of a vector  $\bar{A}$  on a vector  $\bar{B}$  is given by  $\frac{\bar{A} \cdot \bar{B}}{\bar{B} \cdot \bar{B}} \bar{B}$ , while if  $P$  is a plane the projection of  $A$  and  $P$  is given by  $A - \frac{\bar{A} \cdot \bar{B}}{\bar{B} \cdot \bar{B}} \bar{B}$  where  $\bar{B}$  is perpendicular to the plane.

Since, to determine the luminous efficiency, it was necessary to know how much of the beam was being observed, and due to the fact that at times the beam exceeded the limits of the field of view, it was necessary to compute the fraction,  $F$ , of the beam luminescence seen by the telephotometer. To do this we had to make use of the telephotometer angular response function.

The fraction  $F$  is given by

$$F = \frac{\int_B w(s)\rho(s) ds}{\int_B \rho(s) ds} = \frac{\int_B w(s)\rho(s) ds}{P}$$

where the integration is performed with respect to distance over the beam path  $B$ .  $P$  is the practical electron range and  $W(S)$  is a weighting function determined by the angular response function. In the center of the field of view cone  $W=1$ , and as the "shadowy" region at edge of the cone (approximately  $.3^\circ$  from the center) is approached  $W$  decreases and becomes 0 outside the cone. The actual value of  $W$  at a point at an angle  $\alpha$  from the center line of the cone was determined directly from the smoothed angular response function. The smoothing was done using linear segments with the resulting profile having a trapezoidal like appearance.

In computing  $F$ , the integration was performed by making the approximation

$$\int_{S_i}^{S_i + \Delta s} w(s)\rho(s) ds \approx w\left(s_i + \frac{\Delta s}{2}\right) \int_{S_i}^{S_i + \Delta s} \rho(s) ds$$

the latter integral having been computed when the beam length was determined. In this analysis, a scale penetration function equal to unity was assumed along the entire beam length. If a more sophisticated penetration function had been used  $W$  would have had to have been altered to reflect it.

To examine the field of view effects on the slow  $0(1S) 5577\text{\AA}$  luminescent decay we computed the "look time" for the rocket and the beam tip. The look time for the rocket is the time it took for it to go from the edge of the observed field of view to its viewed position, one miliradian above the center of the field of view.

The computation proceeded as follows. The entire field of view was approximately  $.3^\circ$ . So letting  $\beta = \cos(.3^\circ)$  and solving for  $t = T < t_0$  such that the cosine of the angle between  $\bar{N}(t_0)$  and  $\bar{R}(T)$  is  $\beta$  results in the time  $T$  at which the rocket was at the edge of the view field. Hence, the look time at  $t_0$  is  $t_0 - T$ . Since the cosine of the angle between  $\bar{N}(t_0)$  and  $\bar{R}(t)$  is

$$\frac{\bar{N}(t_0) \cdot \bar{R}(t)}{|\bar{N}(t_0)| |\bar{R}(t)|}$$

$T$  was found by solving

$$\bar{N}(t_0) \cdot \bar{R}(t) = \beta |\bar{N}(t_0)| |\bar{R}(t)|.$$

The equation was solved iteratively by using the bisection method. The look time for the beam tip was computed in an analogous way.

To determine the excitation duration of a given atmospheric volume element, it was necessary to compute the velocity components of the rocket both parallel and perpendicular to the magnetic field.

If  $\bar{X}$  is parallel to the magnetic field then

$$v_x(T) = \frac{d\bar{R}}{dt} \cdot \frac{\bar{X}}{|\bar{X}|} \quad \text{gives the}$$

component of velocity in the  $\bar{X}$  direction. The perpendicular component is given by

$$v_y(T) = \frac{d\bar{R}}{dt} \cdot \frac{\bar{Y}}{|\bar{Y}|}$$

$$\bar{Y} = \frac{d\bar{R}}{dt} - v_x(T) \frac{\bar{X}}{|\bar{X}|}.$$

These formulas were used in the computation.

The total power emitted by the electron accelerator was determined by transforming the digitized telemetry data into volts and amperes, and this was then combined with the telephotometer ground based measurements and the values of  $F$  to determine what fraction of the electron beam power was radiated in the  $N_2^+$  first negative.

This parameter  $\epsilon$  is defined as the induced luminous efficiency

$$\epsilon = \frac{(\text{TM volts}) \times |\bar{R}|^2 \cdot 2.32 \times 10^{-14}}{\text{P.T.F.}}$$

TM volts is equal to the 3914Å signal level of the telephotometer, P is the total power,  $T = e^{-0.451 \csc \theta}$  is the atmospheric transmission, and  $\theta$  the elevation angle. Note that the constant 0.451 is the wavelength dependent extinction coefficient and will vary for the different wavelength of interest. The value of  $\epsilon$  for the  $N_2^+$  1N in 3914Å emission vs. altitude is shown in Figure 4.4.

Finally, program INRATIO calculates the intensity ratio of 5577Å to 3914Å emissions,  $\Delta \frac{5577\text{Å}}{3914\text{Å}}$ . This is done by using the following equation:

$$\Delta \frac{5577}{3914} = \frac{R_{5577}}{R_{3914}} = \frac{(\text{TM Volts } 5577) \times 10.6 \times e^{-0.451 \csc \theta}}{(\text{TM Volts } 3914) \times 12.2 \times e^{-0.188 \csc \theta}}$$

where R is in the unit of photon/sec and  $\theta$  is the elevation angle. The constants 10.6 and 12.2 are used to convert TM volts to the actual parameter being measured. The altitudinal variation of the telephotometer intensity ratio is computed and plotted.

#### 4.3 Modular Design

The data reduction and processing system for the rocket borne electron accelerator experiments was designed under certain specific demands. From time to time, the experimental design, apparatus, and the data acquisition format, etc. will be varied and suited for different scientific goals.

This processing system was developed using a general modular design, in anticipation of changing research requirements. Modifications to the experiment design and required data analysis will be made in the enlightenment of information obtained from earlier flights. This system was written with the knowledge that changes will be made, and the modular techniques chosen makes the system more flexible and amenable to ongoing changes in research requirements.

PRECEDE MEASUREMENT OF  $N_2^+$  IN 3914 Å  
LUMINOUS EFFICIENCY

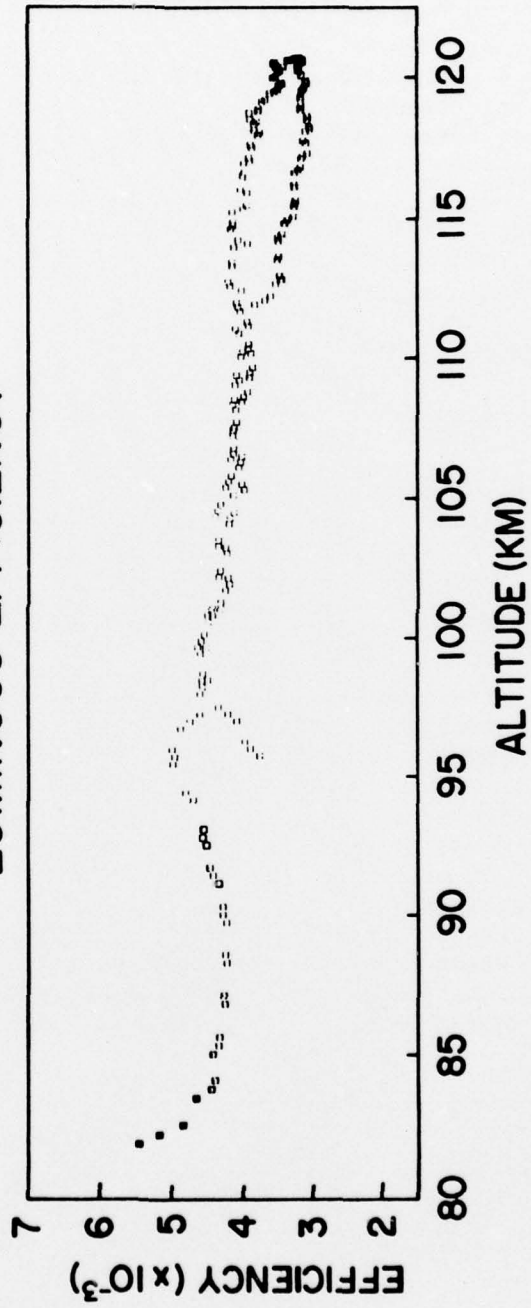


Figure 4.4